

Spatial, Temporal and Chemical Characteristics  
of Airborne Particulate Matter in Phnom Penh, Cambodia

By

Joel D. Bernosky

An Abstract of a Thesis  
in  
Multidisciplinary School

Submitted in Partial Fulfillment  
of the Requirements  
for the Degree of

Master of Science

March 2009

Buffalo State College  
State University of New York  
Department of Geography

## ABSRTACT OF THESIS

### Spatial, Temporal and Chemical Characteristics of Airborne Particulate Matter in Phnom Penh, Cambodia

Phnom Penh, Cambodia is experiencing increased levels of airborne particulates that is attributed to rising population, and in turn larger numbers of vehicles on the road. Vehicles provide fine fraction particulates in the form of exhaust, while also resuspending coarse particles from the road into the air. The objective of this was to examine particulate characteristics by using measurements, observations and summary statistics. Particles were counted and sorted spatially and temporally using two laser particle counters capable of sorting particles into six-channel (0.3, 0.5, 0.7, 1.0, 2.0, and 5.0  $\mu\text{m}$ ) and one channel ( $\leq 10 \mu\text{m}$ ) size fractions. A high-volume air sampler was used to measure particulate mass for comparison with concentrations recorded by the particle counters. Soil grab samples from both urban and rural settings along with collected bulk deposition material were chemically analyzed using a FPXRF unit. This study attributes fine fraction particulates to vehicular sources and coarse fraction particulates to resuspended road dust. The particulate concentrations follow three distinct traffic patterns representative of spatial location within the city. Using enrichment factors, urban particulates are shown to derive from the transport of rural dust into the city, and the urban dust into the air by resuspension.

---

Joel Bernosky

---

Date

Buffalo State College  
State University of New York

Spatial, Temporal and Chemical Characteristics  
of Airborne Particulate Matter in Phnom Penh, Cambodia

A Thesis in  
Multidisciplinary School

By

Joel D. Bernosky

Submitted in Partial Fulfillment  
of the Requirements  
for the Degree of

Master of Science

March 2009

Dates of Approval:

---

---

Stephen J. Vermette  
Professor, Geography & Planning  
Chairperson of the Committee  
Thesis Advisor

---

---

Kevin Railey, Ph.D.  
Associate Provost and Dean of the Graduate School

THESIS COMMITTEE SIGNATORY

Dates of Approval:

---

---

Stephen J. Vermette

Professor, Geography & Planning

---

---

Kim N. Irvine

Professor, Geography & Planning

---

---

Susan Keller-Mathers

Professor, Center for Studies in Creativity

## Acknowledgements

I would like to thank my thesis advisor Dr. Stephen Vermette for piloting the idea for this thesis, providing guidance in the lab and the field, teaching me everything I know about particulates and who along with Dr. Kim Irvine introduced me to Southeast Asia.

I would also like to thank Doug Graber-Nuefeld in helping to take samples and providing transportation on his moto, Sothea for organizing the bulk deposition collection, and his students Sotheavan, Sokeng and Socheat for carrying out the bulk sampling for seven weeks.

I would also like to thank everyone's favorite moto driver Phros for endlessly shuttling me around on his moto to sample sites or restaurants. He also provided some much-needed comic relief in the field.

Dr. Micky Samson of RDIC provided transportation, logistical and gastronomic support. Micky also helped get some of the broken equipment fixed so that it could be used with minimum delay.

Dr. Elisa Bergslien provided the XRF equipment and her expertise of the subject.

I would like to acknowledge my friend and fellow grad student Joseph Gould who was unknowingly participating in competitive thesis writing against me, and for making me feel guilty when I was not working on my paper and he was diligently working on his.

Thanks to my parents Shelley and Dave for support, and my sister Kim for insight and advice on grad school and giving me something to look up to.

Thanks lastly to my fiancée Melissa who put up with my long absences while I was in Cambodia, and provided unending support during the writing of this thesis.

Without the expertise and support of the above, this thesis would not have been possible.

## Table of Contents

	<u>Page</u>
List of Figures	vi
List of Tables	x
Definition of Terms	xi
Chapter 1 – Introduction	1
1.1 Statement of the Problem	1
1.2 Scope and Objectives of this Study	4
Chapter 2 - Literature Review	5
2.1 Cambodia’s Setting	5
2.2 Atmospheric Particulates	8
2.3 Particle Size Fractions and Sources	10
2.3.1 Coarse Particles ( $2.5 \mu\text{m} < D_a < 10 \mu\text{m}$ )	10
2.3.2 Fine Particles ( $D_a < 2.5 \mu\text{m}$ )	11
2.4 Air Quality Standards	12
2.4.1 United States Environmental Protection Agency	13
2.4.2 World Health Organization	15
2.5 Health Hazards	15
2.6 Review of Previous Studies	16
2.6.1 Studies Abroad	16
2.6.2 Studies in Southeast Asia	17
Chapter 3 – Methods and Materials	20
3.1 Global Positioning System	20
3.2 Particle Counters	20
3.3 Particle Counting	24
3.3.1 Spatial Particle Counting	24
3.3.2 Temporal Particle Sampling	26
a. Comfort Star	27
b. Russian Boulevard	28
c. Monivong and Sihanouk Boulevards	28
d. Central Market	28
e. Waterfront	28
f. Mao Tse Toung Boulevard	29
g. Olympic Stadium	29
h. Russian Blvd & Street 315	29
3.3.3 Rural Particle Samples	30
3.3.4 Bangkok Particle Samples	30
3.3.5 Analytical Methods	30
3.4 High-Volume Air Sampler	32
3.4.1 Analytical Methods	34

## Table of Contents Continued...

	<u>Page</u>
3.5 Surface Dust/Dirt Samples and Bulk Deposition Analysis	36
3.3.1 Surface Dust/Dirt Samples	36
3.5.2 Bulk Deposition Analysis	36
3.5.3 Elemental Composition Analysis	36
3.5.4 Enrichment Factors	39
Chapter 4 – Results and Discussion	41
4.1 Spatial Particulate Characteristics	41
4.1.1 Dry Season Particulate Characteristics	41
4.1.2 Rural Particle Counts	46
4.2 Wet vs. Dry Season Particulate Characterizations	47
4.2.1 Wet Season Particulate Characteristics	47
4.2.2 Size Fraction Contributions	50
4.3 Temporal Particle Count Profiles	63
4.4 Particle Mass and Number Count Correlation	68
4.5 Road Dust Elemental Composition	82
4.5.1 Enrichment Factors	83
Chapter 5 – Observations of Particulates in Cambodia	86
5.1 Urban Particulate Observations	86
5.2 Rural Particulate Observations	89
Chapter 6 – Summary and Conclusion	91
6.1 Summary and Conclusion	91
6.2 Recommendations for Further Study	95
References	96

## List of Figures

<u>Figure</u>		<u>Page</u>
1.1	Map of Cambodia Showing Location of Major Cities (Martins, 2005)	3
2.1	Scanning electron microscope photograph of coarse dust particles from the Sahara (Martins, 2005).	10
2.2	Scanning electron microscope photograph of fine smoke particles from the Amazon (Martins, 2005).	12
3.1	Garmin eTrex GPS Unit (Garmin, 2008)	20
3.2	Met One Model 229 One-Channel Laser Particle Counter	22
3.3	Met One Model 237 Six-Channel Laser Particle Counter	22
3.4	Schematic of a Laser Particle Counter's Optics (BPA, 2008)	23
3.5	88 Spatial Sampling Sites	25
3.6	Temporal Sampling Sites in Phnom Penh	27
3.7	Photograph of the Portable High Volume Air Sampler	32
3.8	Close-up Photograph of the Portable High Volume Sampler at RUPP	34
3.9	Photograph of the Portable High Volume Sampler in situ at RUPP	34
3.10	Diagram of Electron Behavior During XRF analysis (Niton, 2008).	39
3.11	Spectral Image for Monivong Boulevard Comfort Star Hotel Road Dust Sample	38
4.1	Fine Particulates in Phnom Penh	42
4.2	Garbage Dump in Phnom Penh	43
4.3	Coarse Particulates in Phnom Penh	44
4.4	Fine Particulates by Road Surface in Phnom Penh	45

### List of Figures Continued...

<u>Figure</u>		<u>Page</u>
4.4	Coarse Particulates by Road Surface in Phnom Penh	46
4.6	Mean Particle Counts for PM <sub>10</sub> at Sample Sites at Urban and Rural Sites	48
4.7	Temporal Particle Counts for Particles $\leq 10 \mu\text{m}$ and $0.3\text{-}5.0 \mu\text{m}$ at Olympic Stadium Location on June 22, 2008	51
4.8	Normalized Temporal Particle Counts Comparing Particles $\leq 10 \mu\text{m}$ and $0.3\text{-}5.0 \mu\text{m}$ on June 22, 2008 at the Olympic Stadium Location	52
4.9	Temporal Particle Counts for Particles $\leq 10 \mu\text{m}$ and $0.3\text{-}5.0 \mu\text{m}$ at Monivong Boulevard Comfort Star Hotel Location on June 22, 2008	53
4.10	Normalized Temporal Particle Counts Comparing Particles $\leq 10 \mu\text{m}$ and $0.3\text{-}5.0 \mu\text{m}$ on June 22, 2008 at the Comfort Location	54
4.11	Temporal Particle Counts for Particles $\leq 10 \mu\text{m}$ and $0.3\text{-}5.0 \mu\text{m}$ at Monivong Boulevard Comfort Star Hotel Location on June 23, 2008	55
4.12	Normalized Temporal Particle Counts Comparing Particles $\leq 10 \mu\text{m}$ and $0.3\text{-}5.0 \mu\text{m}$ on June 23, 2008 Samples at the Comfort Location	56
4.13	Average Percent Contributions for Particles sized $0.3\text{-}5.0 \mu\text{m}$ at the Olympic Stadium Location on June 22, 2008	57
4.14	Average Percent Contributions for Particles sized $0.3\text{-}5.0 \mu\text{m}$ at the Monivong Boulevard Comfort Star Location on June 22, 2008	58
4.15	Average Percent Contributions for Particles sized $0.3\text{-}5.0 \mu\text{m}$ at the Monivong Boulevard Comfort Star Location on June 23, 2008	59
4.16	Average Temporal Percent Contributions for Particles sized $0.3\text{-}5.0 \mu\text{m}$ at the Olympic Stadium Location on June 22, 2008	60

### List of Figures Continued...

<u>Figure</u>		<u>Page</u>
4.17	Average Temporal Percent Contributions for Particles sized 0.3-5.0 $\mu\text{m}$ at the Monivong Boulevard Comfort Star Location on June 22, 2008	61
4.18	Average Temporal Percent Contributions for Particles sized 0.3-5.0 $\mu\text{m}$ at the Monivong Boulevard Comfort Star Location on June 23, 2008	62
4.19	Temporal Particle Counts for Monivong Boulevard Comfort Star Location on June 15, 2008	64
4.20	Temporal Particle Counts for Monivong Boulevard Comfort Star Location on June 20, 2008	66
4.21	Temporal Particle Counts for Intersection of Monivong and Sihanouk Boulevard Location on June 17, 2008	67
4.22	Temporal Particle Counts for Russian Boulevard Location on June 17, 2008	69
4.23	Temporal Particle Counts for Central Market Location on June 20, 2008	71
4.24	Temporal Particle Counts for Waterfront Location on June 20, 2008	72
4.25	Temporal Particle Counts for Mao Tse Toung Location on June 21, 2008	74
4.26	Temporal Particle Counts for Olympic Stadium Location on June 21, 2008	75
4.27	Temporal Particle Counts for Russian Blvd. & Street 315 Location on June 21, 2008	76
4.28	Particle Mass and Number Count Correlation	80
4.29	Temporal Particle Mass Measurements for Monivong Boulevard Comfort Star Location on June 15, 2008	81

## List of Figures Continued...

<u>Figure</u>		<u>Page</u>
4.30	Elemental Composition of Urban and Rural Road Dust Samples	82
5.1	A City Worker Sweeping Dust and Garbage Debris from a Street in Phnom Penh	86
5.2	Commuters in Phnom Penh Wearing Masks to Protect from Particulate Inhalation	87
5.3	Dust Buildup on Two Roads in Outer-Phnom Penh	88
5.4	An Unpaved Side Street in Phnom Penh	89
5.5	A Dirt Road Outside Phnom Penh	90
5.6	A Dirt Road in a Remote Rural Village	90

## List of Tables

<u>Table</u>		<u>Page</u>
2.1	U.S. EPA Primary Standard vs. WHO Guidelines for PM <sub>2.5</sub> and PM <sub>10</sub>	15
4.1	Particle Counts for PM <sub>10</sub> at Sample Area in Urban and Rural Phnom Penh	49
4.2	Percent Contribution of Particle Size Fractions	63
4.3	Mean, median and standard deviation of PM <sub>10</sub> particle counts	77
4.4	Start, End and Total Mean Particle Counts for High-Volume Sampler Runs	79
4.5	Mean Urban, Rural and Global Crustal Abundance of Measured Elements in ppm	83
4.6	Mean concentration in ppm of Urban, Rural and Bulk Deposition Material	84
4.7	Enrichment Factors for Urban Road Dust Using Rural Road Dust as Reference Material and Arsenic as Reference Element	84
4.8	Enrichment Factors for Bulk Deposition Material Using Urban Road Dust as Reference Material and Arsenic as Reference Element	85

## Definition of Terms

$D_a$	:	Aerodynamic Diameter
FPXRF	:	Field Portable X-Ray Fluorescence Unit
GDP	:	Gross Domestic Product
g/L	:	Grams per Liter
GNP	:	Gross National Product
GPS	:	Global Positioning System
KeV	:	Electron Volts
L/min	:	Liters per Minute
$m^3/min$	:	Cubic meters per Minute
PM	:	Particulate Matter
PM10	:	Particulate Matter $D_a \leq 10\mu m$
PM2.5	:	Particulate Matter $D_a \leq 2.5\mu m$
PM <sub>x</sub>	:	Particulate Matter $D_a \leq x$
PPM	:	Parts per Million
RUPP	:	Royal University of Phnom Penh
TSP	:	Total Suspended Particulates
$\mu m$	:	Micrometers
UTM	:	Universal Transverse Mercator
U.S. EPA	:	United States Environmental Protection Agency
WGS84	:	World Geodetic System 84
WHO	:	World Health Organization



## **Chapter 1 - Introduction**

### **1.1 Statement of the Problem**

Southeast Asia, with Cambodia in particular, lacks many detailed studies concerning air quality, and studies concerning the spatial and temporal trends of ambient particle pollution are rarer still. An understanding of the trends and behaviors of particle pollution is needed as development in Southeast Asian countries continues. Particle pollution plays a role not only as an aesthetic detractor and respiratory irritant, but has also been shown to have negative effects on health. Airborne particulates pose specific health threats to urban populations in large concentrations. Epidemiological studies show a positive correlation between high levels of fine fraction ambient particle pollution and adverse health effects such as respiratory and cardiovascular disease and acute mortality (Spirn, 1985; Pope et al., 1995).

While little attention has been given to Southeast Asia concerning air quality, numerous studies have been carried out in nearby countries such as India, Japan, and China (Dasgupta S. et al., 2005). The significant interest in these largely developed nations suggests that as development accelerates and populations grow, more awareness and resources are given to the study and control of airborne particulates. Because of Cambodia's status as a developing nation and its (and Southeast Asia's) recent violent political history, scientific studies have been few and far-between. The lack of significant air quality data in Cambodia and Southeast Asia leaves a considerably fast growing section of Asia unrepresented. Air quality monitoring and control in Cambodia, because of its status as a developing nation, is rare and if performed, proprietary. Cambodia lacks

many restrictions on pollution control that developed nations mandate such as emissions standards for vehicles and commercial industries.

After nearly three decades of war and internal struggles, Cambodia remains one of the poorest nations in the world with a Gross National Product (GNP) Per Capita of approximately US\$300. Agriculture remains a large industry, accounting for ~50% of Cambodia's Gross Domestic Product (GDP). The Agriculture industry is largely conducted in rural areas, where ~80% of Cambodia's population resides (World Bank, 2005). Cambodia has seen its GDP nearly double its growth rate from 3.5% to 5.9% from 1996 to 2001 (United Nations, 2005). Because of the growth in Cambodia's population and economy, growth in pollution-creating anthropogenic activities is also increasing.

The city of Phnom Penh (13°N, 105°E) is located in south-central Cambodia (Figure 1.1), at the confluence of the Bassac, Mekong and Tonle Sap rivers. The city is located on the West side of this confluence. With a population of over one million, Phnom Penh covers approximately 375 square kilometers (Planning, 2004). While still undergoing heavy development and population expansion, Phnom Penh is surrounded on all sides by rural farmland. Phnom Penh, the capital city, is also expanding its boundaries as a result to the recent influx of population from the provinces and the country's GDP growth. The expansion of Phnom Penh carries with it increased energy and resource use as well as increased vehicles and traffic (Furuuchi et al., 2006).

Particle pollution in Phnom Penh is a significant problem, as many visitors to the city remark on the dust levels, as they can be the first and lasting impression of the environment as seen in travel accounts with names such as *Dust, dust and some more*

*dust, Phnom Penh, Cambodia* (Stone, P., 2003) and news reports such as *Thousands ill as Phnom Penh air pollution doubles* (Reuters, 2001).



**Figure 1.1 – Map of Cambodia Showing Location of Major Cities (CIA, 2008)**

Ambient particulates are being increasingly studied worldwide due to recent evidence of increased mortality and other negative health effects associated with elevated levels of ambient particles. The most common form of particulate matter (PM) measurement is particle mass loadings derived from using either gravimetric methods or high volume air samplers and this is reflected in both the literature and PM standards set by organizations such as the United States Environmental Protection Agency (U.S. EPA) or World Health Organization (WHO). A less common way to measure PM concentrations is by using a laser particle counter to measure particle number counts because laser particle counters tend to be more expensive than other forms of PM analysis devices and because they have only been in existence for approximately the last few decades.

## 1.2 Scope and Objectives of this Study

Much of the business in Phnom Penh is conducted at shops on street level. Most homes in Phnom Penh are at street level, but some are at a maximum of six stories, so correspondingly, most citizens are exposed to constant street level pollution for the majority of the day. Because of this, along with the relative dearth of air quality data available for Phnom Penh, field-sampling sites were selected to be representative of the ambient particle pollution a resident of Phnom Penh would experience.

Field sampling was carried out in Phnom Penh, Cambodia from January 15 to 17, 2007, June 19, 2007 and June 15 to 24, 2008. By employing the use of a high volume air sampler, a one-channel laser particle counter to measure particles  $\leq 10 \mu\text{m}$ , and a six-channel laser particle counter to measure particles  $0.3 - 5.0 \mu\text{m}$ , this study aims to characterize the spatial and temporal trends and variability of ambient particulate matter in Phnom Penh, and to discern the general sources of the particulate matter.

The first section of this study examines the temporal aspects of PM matter in Phnom Penh by using both one and six-channel laser particle counters as well as the high-volume sampler over a given time period in order to derive mass loadings and particle counts for various locations in the city. The second section of this study examines the spatial variability of PM using the six-channel laser particle counter in Phnom Penh over 88 sites in two different seasons (the dry and rainy seasons).

## Chapter 2 - Literature Review

### 2.1 Cambodia's Setting

Atmospheric monitoring for a variety of parameters are typically carried out in developed nations, however, many developing nations in Central and South America and especially Asia lack sufficient investment and commitment to air quality monitoring. While some nations such as China, Brazil and Mexico have begun to routinely monitor air quality, monitoring is still uneven and not ubiquitous (Wheeler, 2001). Studies of ambient particulate matter concentrations in Asia are rare, and particle count studies are rarer still (Tippayawong et al., 2006).

Developing nations are home to a large amount of factories and other industrial emitters of pollutants, and while factories with zero control on emissions certainly exist, many developing nations are beginning to adopt standards and regulations on point source industrial emissions, following the example of developed nations (Hettige, 1996).

Around 50% of the world's population lives in South and East Asia. This population continues to increase and coupled with an increasing quality of life, air pollution levels are continuing to rise as demand for energy and transportation increases, especially in urban areas. In rural areas in this part of the world the burning of biofuels such as wood and charcoal is a major source of pollution (Lelieveld et al., 2001, United Nations, 2005).

Cambodia covers an area of 181,040 km<sup>2</sup>, an area just smaller than the state of Oklahoma (CIA, 2008). Cambodia's physiographic setting includes relatively flat plains and mountainous terrain in the southwest and north (CIA, 2008). The lowland plains and the Mekong and Tonle Sap basins are prone to seasonal flooding during the monsoon

season (May to November), and primarily are composed of alluvium deposits which can exceed thicknesses of 200 meters in some areas (Feldman & Rosenboom, 2001, as cited in Irvine, 2006). Alluvium deposits are composed mainly of loose material that can be easily suspended into the air by wind erosion. The fluvial morphology of the Tonle Sap, Mekong and Bassac Rivers has significant impacts on Phnom Penh. The banks of the Bassac River in Southern Phnom Penh are migrating east, eroding the eastern banks and expanding the western banks, while the Bassac's mixing with the Tonle Sap and Mekong rivers result in the deposition of large levels of coarse alluvial sand (Molyvann, 2003). The deposition of alluvial sand at the meeting point of the mixing rivers is periodically dredged and used as fill for Phnom Penh's further expansion into its surrounding wetlands, effectively transporting the coarse sandy soil to locations away from the rivers.

The flooding of the rivers in the wet season plays a crucial role not only in Cambodia's agricultural productivity, but also in shaping the geomorphology of the country. The riverbanks around Phnom Penh are naturally formed from the deposition of sandy alluvial sediment, and reinforced by anthropogenic means. The riverbanks in Phnom Penh tend to be higher than the average height of flood waters in the Tonle Sap and Bassac Rivers; around 12 meters in height (Molyvann, 2003). During the dry season, the rivers recede and can expose up to ten of the twelve meters the reinforced riverbanks. The sides of riverbanks and low lying fields directly bordering the rivers contain a finer alluvial sediment with higher clay contents and lower sand and gravel contents than the sandy alluvial sediment. This sediment accumulates in deep nutrient-rich deposits. Heavier clay soils are found in floodplains further away from the rivers. This soil is more homologous than the two previously discussed; as distance from the flooding rivers

increased, flow energy decreased, allowing for the deposition of finer sediment (Molyvann, 2003).

Phnom Penh is particularly susceptible to flooding. Because of its recent expansion, much of the city has been extended beyond the original riverbanks into plains below flood level. A series of concentric dikes have been constructed around parts of the city, but because of Phnom Penh's rapid growth and high cost of construction, the dikes cannot possibly protect the entire city from floodwaters. During a flood, up to two-thirds of Phnom Penh can be flooded, causing the city to effectively shut down (Molyvann, 2003).

Major sources of air pollution in Phnom Penh are from the approximately 170 factories, 63,000 cars trucks and buses and 450,000 motorbikes in use (United Nations, 2002). United Nations (2002) also reports that industrial and urban pollution sources, while a factor, are not yet of major concern in Phnom Penh (United Nations, 2002). The 170 factories are mostly in the garment industry, although factories for smaller industries such as food and beverage, construction materials, brick-making and rubber manufacturing exist in small quantities (United Nations, 2005). Factories in Phnom Penh typically use aged technologies without pollution controls. Private power generators have increasingly augmented an unreliable power grid in virtually every business in the service industry (World Bank, 2005; United Nations, 2005). Motorbikes in Phnom Penh are generally secondhand imported models, which consume more fuel and have higher emissions than their modern counterparts. Frequent traffic jams due to increased population and in turn increased amounts of vehicles can lead to high concentrations of emissions (United Nations, 2005).

Coarse particulates are another major source of air pollution in Phnom Penh, and are derived from material re-entrained from a large number of unpaved roads in the city, or poor management of construction materials. Other major sources of re-suspended coarse material include alluvial sediment, sand, soil, gravel, and cement (Fraser et al., 2003; United Nations, 2005). Central Cambodia is situated in a valley running northwest to southeast carved by the Tonle Sap and Mekong Rivers. The eastern edge of the valley contains two hills composed of Jurassic age sandstone formed from past alluvial deposits. The rugged terrain in north Cambodia contains sandy soils from the erosion of sandstone hills that can reach heights of 100 meters. The low-lying plains contain soils rich in clays (Molyvann, 2003).

## **2.2 Atmospheric Particulates**

Urban air pollution is regarded as a heterogeneous mixture of anthropogenic and natural pollutants. The particles differ by factors such as size and chemical composition, depending on the particle's source (Schwartz & Neas, 2000). Most cities experience high levels of particulate matter (PM), however even in situations where air quality is considered acceptable (within government standards), regional factors such as the city's physiographic setting and urban landscape can cause street level pollution to reach levels that may be harmful to humans (Spirn, 1985). Dense building arrangement creates microclimatic variations in temperature and ventilation, which may arbitrarily heighten pollution concentrations in street canyons (Murena & Favale, 2006; Niachou et al., 2008).

Recently, with the promotion of fossil fuels like heating oil and natural gas over coal for heating in cities, particle pollution has seen a decrease in concentrations. Offsetting this decrease however is ever-growing population and vehicular traffic

associated with cities (Manoli et al., 2002). Manoli et al., (2002) also points out that while car emissions are raising particulate levels in cities, the particles they emit are also finer than those emitted by coal plants, resulting in an increase in breathable fine fraction particulates.

Ambient particles exist in the atmosphere in a bimodal distribution encompassing both fine (defined in this study as particles  $\leq 2.5 \mu\text{m}$ ) and coarse size fractions (defined in this study as particles 2.5 to 10.0  $\mu\text{m}$ ) (Manoli et al., 2002). Gomiscek et al., (2004) notes that because natural sources of PM exist, controlling ambient PM levels can be difficult, especially if they are part of the natural background level (pollutants from local, natural sources).

Studies have shown very strong evidence that resuspended dust is a major contributor to ambient particulates in urban environments. Studies conducted in Granite City, Illinois by Glover et al. (1989) and in Hamilton, Ontario by Vermette et al. (1988) show links between resuspended road dust and collected ambient air samples.

Concern has been expressed over the health implications for large quantities of these particulates, which has led to multiple epidemiologic studies being carried out to study the effects on the inhalation of particulates on humans (Spirn, 1985; Pope et al., 1995). In recent years, most research has been conducted on fine particles because of their increased ability to enter deep lung tissue and ability to travel long distances (Manoli et al., 2002).

## 2.3 Particle Size Fractions and Sources

### 2.3.1 Coarse Particles ( $2.5 \mu\text{m} < D_a < 10 \mu\text{m}$ )

Coarse particles are generally associated with natural sources such as forest and grassland fires, deforestation, crustal material and oceanic spray (Diner et al., 2004; Manoli et al., 2002). Coarse particles, because of their natural sources, are generally jagged and irregular in shape (Venkataraman, 1999). Figure 2.1 shows coarse Saharan dust particles collected on a membrane filter. The particles appear rough and flaky and represent a variety of different shapes.

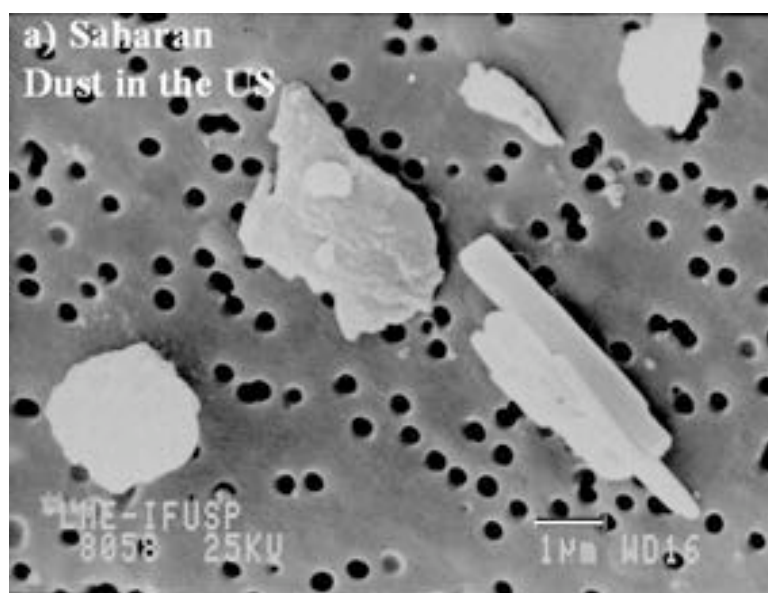


**Figure 2.1 – Scanning electron microscope photograph of coarse dust particles from the Sahara (Martins, 2005).**

A study carried out by Koulouri et al., (2008) in the Eastern Mediterranean showed that the total mass of fine fraction particles (defined in the study as  $D_a < 1.3 \mu\text{m}$ ) for both natural and anthropogenic sources was approximately equal at around 40% each.

In comparison, the same study was able to apportion 60% of the total mass of the coarse particles (defined as  $1.3 \mu\text{m} < D_a < 10 \mu\text{m}$ , respectively) to natural sources.

Source apportionment studies show that a majority of coarse particles (particles  $>2.5\mu\text{m}$ ) are from re-suspension of soil, and road dust (Fraser et al, 2003; Manoli et al., 2002). Manoli et al. (2002), in a study conducted in Greece found a strong correlation between coarse particles and road dust. This correlation suggests that re-suspended road dust is a major contributor to the coarse fraction of ambient particulates by also showing that re-suspended road dust dominated the coarse size fraction at 57% of the total mass.

### **2.3.2 Fine Particles ( $D_a < 2.5 \mu\text{m}$ )**

Fine particles originate mostly from anthropogenic emissions; however, a small percentage of fine particles may originate from natural processes such as high temperature forest fires. In general, the smaller the particle, the higher the heat required to create it, so very fine submicron particles can be attributed to anthropogenic means.

Fine particles are produced from combustion sources such as traffic exhaust (Srivastava & Jain, 2006; Seinfeld, 1986; Wu et al., 2007). Fine particles derived from emissions or high temperature burning sources display a round or nearly spherical shape (Seames, 2003). Figure 2.2 shows a scanning electron microscope photograph of smoldering phase smoke from the Amazon from anthropogenic burning of trees. The particles appear to be round, and care must be taken to distinguish the lighter colored particles from the dark pore holes in the membrane filter that the particles sit on.

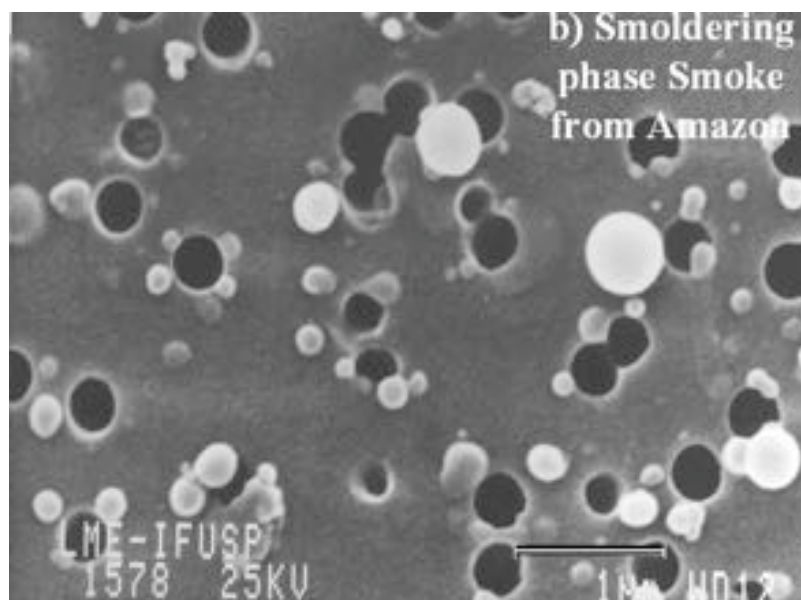


**Figure 2.2 – Scanning electron microscope photograph of fine smoke particles from the Amazon (Martins, 2005).**

Gehrig & Buchmann (2003) note however that the coarser  $PM_{10}$  and finer  $PM_{2.5}$ , may contain some re-suspended natural material in addition to the ambient anthropogenic particles. Manoli et al. (2002) found in a study conducted in Greece that 38% of fine particles could be apportioned to traffic exhaust while 28% could be apportioned to re-suspension of road dust.

Fine particulates have been shown to be found in more homologous groupings, as they tend to travel further in the atmosphere and stay suspended in the atmosphere longer than their coarse counterparts, which tend to settle out gravimetrically fairly soon after introduction or re-suspension (Gehrig & Buchmann 2003).

## **2.4 Air Quality Standards**

Suspended particulates in ambient air pose a significant threat to the health and wellness of millions of people living in urban areas. As populations and development

pace increase around the world, anthropogenic emissions increase, along with negative health effects on citizens. Ambient particle pollution is known to be a good outdoor air quality indicator, and is represented in scientific studies in three major groups, total suspended particulates (TSP), Coarse Particles  $\leq 10 \mu\text{m}$  ( $\text{PM}_{10}$ ), and Fine Particles  $\leq 2.5 \mu\text{m}$  ( $\text{PM}_{2.5}$ ) (Fromme et al., 2008). These three major classifications of particulate matter (PM) represent the categories of PM used in legislation by the United States Environmental Protection Agency (U.S. EPA) and world bodies such as the World Health Organization (WHO).

Air quality standards exist to set a maximum allowable limit for pollutants known to be harmful to humans, and in lesser cases the environment at large. A large number of different agencies set particular air quality standards in the United States and abroad. Two of the most widely used standards are those of the U.S. EPA and the WHO.

Air quality standards for TSP and PM typically exist as mass concentrations and size distributions with very little attention paid to particle count number loadings although particle count numbers are good alternatives or supplements to mass loading measurements (Tippayawong et al., 2006). Harrison et al. (1999) suggest that particle count numbers may be better predictors of human health effects than mass concentrations of particles.

#### **2.4.1 United States Environmental Protection Agency**

The U.S. EPA adopted standards for TSP in 1969 as defined in the National Ambient Air Quality Standards (NAAQS) for Particulate Matter in the Clean Air Act (Section 108 [42 U.S.C. 7408] and Section 109 [42 U.S.C. 7409]). The NAAQS established primary and secondary standards for six criteria pollutants: Carbon Monoxide

(CO), Lead (Pb), Nitrogen Dioxide (NO<sub>2</sub>), Ozone (O<sub>3</sub>), Particulate Matter (PM), and Sulfur Dioxide (SO<sub>2</sub>). Primary standards are maximum criteria pollution levels set to protect human health, especially in high-risk people such as the elderly, children, and people with respiratory disease. Secondary standards are in place to protect human quality of life, or public welfare. When criteria pollution levels reach concentrations coinciding with secondary standards, adverse effects such as crop and vegetation, building and ecosystem damage may occur (U.S. EPA, 2007).

The EPA defined TSP as particles up to 25 to 45  $\mu\text{m}$  as collected by a high-volume sampler. The primary standards for TSP levels were set at a 24-hour average of 260  $\mu\text{g}/\text{m}^3$ , while the adopted secondary standard was set at 150  $\mu\text{g}/\text{m}^3$  for a 24-hour average. Both standards were not to be exceeded more than once a year, according to the NAAQS.

In 1979, the EPA brought about the first review of the standards set in the NAAQS document from 1969. The revisions took effect in 1987, effectively trading the TSP standards for PM<sub>10</sub> standards. PM<sub>10</sub> is defined as particles with a diameter less than or equal to 10  $\mu\text{m}$ . The new primary and secondary PM<sub>10</sub> standards were set as at 150  $\mu\text{g}/\text{m}^3$  and 50  $\mu\text{g}/\text{m}^3$  respectively, over a 24 hour average, and not to be exceeded more than once a year (U.S. EPA, 2008).

In 1997 another overhaul of the NAAQS was completed by the U.S. EPA, which further improved the standards for ambient particulates. PM<sub>2.5</sub> (Particles with a diameter less than or equal to 2.5  $\mu\text{m}$ ) standards were added to the legislation however, unlike the previous revision to the NAAQS document, the new PM<sub>2.5</sub> standards did not replace the prior PM<sub>10</sub> standards, they were simply added in order to provide measurements

including both coarse (PM<sub>10</sub>) and fine (PM<sub>2.5</sub>) fractions of respirable ambient particulates. The standards for PM<sub>2.5</sub> were set at 15 µg/m<sup>3</sup> for the annual arithmetic mean and 65 µg/m<sup>3</sup> over a 24-hour average. In 2006 the PM<sub>2.5</sub> standard was further revised by lowering the 24-hour average to 35 µg/m<sup>3</sup> (EPA 2006, EPA 1997).

#### 2.4.2 World Health Organization

The international World Health Organization (WHO) sets air quality guidelines to be followed, as it does not have the authority to impose mandatory standards on sovereign nations the way that the U.S. EPA does inside the United States. Annual mean concentrations for PM<sub>2.5</sub> and PM<sub>10</sub> are 10 and 20 µg/m<sup>3</sup> respectively, while 24-hour averages for PM<sub>2.5</sub> and PM<sub>10</sub> are 25 and 50 µg/m<sup>3</sup> respectively (WHO, 2008). These guidelines are noticeably lower than the current U.S. EPA standards. Table 2.3.2 below shows the U.S. EPA standards alongside the WHO guidelines for comparison.

**Table 2.1 – U.S. EPA Primary Standard vs. WHO Guidelines for PM<sub>2.5</sub> and PM<sub>10</sub>**

	<i>PM<sub>10</sub> Annual Mean</i>	<i>PM<sub>2.5</sub> Annual Mean</i>	<i>PM<sub>10</sub> 24-hour Mean</i>	<i>PM<sub>2.5</sub> 24-hour Mean</i>
U.S. EPA Primary Standard	N/A	15 µg/m <sup>3</sup>	150 µg/m <sup>3</sup>	35 µg/m <sup>3</sup>
WHO Guideline	20 µg/m <sup>3</sup>	10 µg/m <sup>3</sup>	50 µg/m <sup>3</sup>	25 µg/m <sup>3</sup>

#### 2.5 Health Hazards

Numerous epidemiological studies have certified the relationship between ambient air pollution and acute and chronic health effects. Ambient particle pollution has long been linked to negative effects on human health such as decreased lung function, exacerbated asthma, respiratory disease and non-accidental mortality (Pope et al., 1991; Peters et al., 1999; Goldberg et al., 2001; Soukup & Becker, 2000).

Qian et al. (2007) found evidence that PM<sub>10</sub> levels are linked to acute effects on cardiopulmonary mortality, while Wilson and Suh (1997) show that fine particles (PM<sub>2.5</sub>) have more negative health effects than coarser particles (PM<sub>10</sub>). Fine particles tend to travel further into the respiratory tract and are able to inflict alveolar inflammation as well as become lodged in interstitial lung tissue (Seaton et al., 1995). Soukup & Becker (2000) found that PM<sub>2.5-10</sub> deposits preferentially in the bronchial region, and Kim et al. (1996) states that particulates are deposited up to 17 times higher in surface regions of the lungs where bacterial infections and asthma inducers are centered indicating that high particulate levels are a major source of lung-borne bacterial infections and exacerbated asthma.

## **2.6 Review of Previous Studies**

### **2.6.1 Studies Abroad**

Previous studies conducted by in London by Waller (1967) (as cited in Harrison et al., 1999), using electron microscopy, found that natural background levels of TSP had particle counts of 10,000 particles/cm<sup>3</sup> ( $1.00 \times 10^{10}$  particles/m<sup>3</sup>) and 30 – 50,000 particles/cm<sup>3</sup> ( $3.00 \times 10^{10}$  to  $5.00 \times 10^{10}$  particles/m<sup>3</sup>) in streets. A study conducted by Vermette, 2008) in San Salvador, Bahamas, found particle counts ranging from  $3.90 \times 10^7$  to  $6.55 \times 10^7$  particles/m<sup>3</sup>. These low particle counts are due to a prevailing wind that carries clean maritime air to the Bahamas from the Atlantic Ocean. With the nearest major source of air pollution across the entire ocean, the prevailing winds carry relatively clean air.

A study conducted in Erfurt, Germany by Tuch et al. (1997) recorded 180 day average particle counts of  $1.31 \times 10^{10}$  particles/m<sup>3</sup> for particles 0.01-0.1  $\mu\text{m}$ ,  $5.10 \times 10^9$  particles/m<sup>3</sup> for particles 0.1-0.5  $\mu\text{m}$  and  $5.60 \times 10^7$  particles/m<sup>3</sup> for particles 0.1-0.5  $\mu\text{m}$ . This study used an aerosol size spectrometer to record particle mass and number count concentrations. The spectrometer uses two different methods to measure particle mass and number concentrations depending on the size of a particle. Particles 0.01-0.3  $\mu\text{m}$  were classified and sorted with a differential electrical mobility analyzer, a method that sorts based on a particle's spherical diameter, and counted using a condensation particle counter. Particles 0.1-2.5  $\mu\text{m}$  were sorted using an optical particle counter. The authors note that classifications of particles using the optical laser particle counter are dependent on the particle's chemical composition, because particles with different chemical compositions have different refractive properties. The electrical classification (used for particles 0.01-3.0  $\mu\text{m}$ ) was independent of chemical composition. Calculations using data from the optical particle counter were calibrated using the refractive properties of particles identified using the electrical mobility analyzer.

The study found a poor correlation between particle mass concentration and total particle number counts using particle sizes of 0.1 to 2.5  $\mu\text{m}$ . The particle mass and number count measurements correlated with only an  $r^2$  value of 0.50, a correlation that the authors deemed poor.

### **2.6.2 Studies in Southeast Asia**

Tippayawong et al. (2006) recorded 10 hour PM mass concentrations with a low flow high-volume sampler in Chang Mai, Thailand from December 2003 to January

2004. The authors note that winter months were chosen for the study because it is a time of cool, dry air, and also that PM levels tend to be higher.

Using the high-volume sampler with a flow rate of 100 L/min, mass concentrations were found to be 72-290  $\mu\text{g}/\text{m}^3$  with an average mass concentration of  $149 \pm 45 \mu\text{g}/\text{m}^3$ . Their data show that residential areas tend to have lower PM concentrations than urban and industrial areas, and that coarser particle counts (0.3 – 10  $\mu\text{m}$ ) showed very little variation between the four sites sampled.

Tippayawong et al. (2006) also used an optical particle counter that ran simultaneously with a high-volume sampler. The particle counter, with a flow rate of 2.83 L/min recorded number counts in one-minute intervals, with ten minutes between each sample.

The particle sampler recorded particle counts in four size bins: 0.3-0.5, 0.5-1.0, 1.0-5.0 and 5.0-10  $\mu\text{m}$ . Respectively, particle count number concentrations were  $6.60 \times 10^6$ ,  $1.18 \times 10^6$ ,  $2.11 \times 10^5$ , and  $1.12 \times 10^4$  particles/ $\text{m}^3$ . The data collected shows that particles  $D_a < 1.0 \mu\text{m}$  were responsible for over 90% of the total amount of particles recorded.

Temporal variation of particle counts at each site was not significant, and the authors note that no short term peak of particle counts was discernable during rush hour traffic, which was an unexpected outcome due to the over one million registered motorcycles in the city. Particles in the smallest size bin (0.3 – 0.5  $\mu\text{m}$ ) showed slight temporal variation throughout the day. The authors conclude that the majority of vehicles must produce particle emissions lower than the particle counter's detection limit (0.3  $\mu\text{m}$ ). The second and third size bins (0.5 – 1.0  $\mu\text{m}$  and 1.0 – 5.0) displayed larger

variations in particle count with concentrations decreasing throughout the day into the evening. These larger particles may be influenced by local sources such as construction. The fourth size bin (5.0 – 10.0  $\mu\text{m}$ ) did not show a distinct pattern, and remained fairly constant throughout the temporal sampling. Small variations in the particle count for this size bin were attributed to the re-suspension of construction and road dust.

A study carried out in Phnom Penh by Furuuchi et al., (2006) sampled TSP with high volume air samplers and quartz fiber filters. The authors show that high concentrations of TSP were found in residential areas as well as a peninsula on the riverbank. The higher TSP concentrations were caused by the re-suspension of dust from unpaved roads in the residential area and the riverbank. They suggest also that wind over the rivers in Phnom Penh can act to dilute TSP levels near the river, and act as a barrier, preventing inner-city pollution from reaching the riverbank. The authors also found an increase in TSP with air temperature, although the study did not attempt to identify the cause of this relationship.

Takahiro et al., (2006) used a high-volume sampler to collect TSP in Phnom Penh so that concentrations could be calculated. The study found that central downtown TSP concentrations were 100-150  $\mu\text{g}/\text{m}^3$ , and that because the ambient TSP is re-suspended road dust or soil, concentrations were higher during the day than at night because of less traffic flow.

### **Chapter 3 – Methods and Materials**

Airborne ambient pollution samples were collected employing laser particle counters and a high-volume air sampler in the city of Phnom Penh and its rural surroundings. Samples were collected during over two years in the dry season (January 15 to 17, 2007) and wet season (June 19, 2007 and June 15 to 24, 2008). Sampling was carried out in both urban and rural locations. Sample locations for the particle counters were chosen to represent unique site-specific environmental scenarios. Particle samples were used to quantify spatial and temporal variability in Phnom Penh and spatial variability in nearby rural areas. Road dust samples were collected in both urban and rural environments for elemental analysis with an x-ray fluorescence unit. An analysis based on observations was also conducted in the study area.

#### **3.1 Global Positioning System**

A hand-held Global Positioning System (GPS) unit (Garmin eTrex; Figure 3.1) was used to record location data. Universal Transverse Mercator (UTM) coordinates were used along with World Geodetic System (WGS) 84 datum. The WGS84 datum is simply a coordinate grid superimposed on a spheroid to translate recorded location data into real-world position taking into account the earth's ellipsoid shape.

GPS units use a network of 24 to 32 microwave-transmitting satellites to triangulate location using a minimum of four satellites. Location accuracy, using the e-trex GPS ranged from 8-20 meters. Locations nearer the city center generally had higher margins of error, as GPS units tend have trouble accurately identifying coordinates when the sky is obscured from satellites. The site-specific coordinates were used to plot site

locations and air particulate counts on geo-referenced Google Earth maps. Locations were plotted on Google Earth by converting the UTM coordinates to Latitude and Longitude coordinates and manually typing the coordinates into Google Earth.



Figure 3.1 – Garmin eTrex GPS Unit (Garmin, 2008)

### 3.2 Particle Counters

A battery operated one-channel particle counter, capable of measuring ambient particles  $\leq 10 \mu\text{m}$  (Met One Model 229-.3 [Figure 3.2]), and a battery operated six-channel (Met One Model 237 [Figure 3.3]) particle counter, capable of measuring and sorting ambient particles with an aerodynamic diameter ( $D_a$ ) of 0.3, 0.5, 0.7, 1.0, 2.0 and 5.0  $\mu\text{m}$  were used to sample air quality.



**Figure 3.2 – Met One Model 229 One-Channel Laser Particle Counter**



**Figure 3.3 - Met One Model 237 Six-Channel Laser Particle Counter**

The one-channel particle counter provides a single reading or a count of all particles less than or equal to 10  $\mu\text{m}$  ( $\text{PM}_{10}$ ). The six-channel particle counter's output is shown as six individual readings, one for each channel or size range. Particles up to 0.3  $\mu\text{m}$  in size are represented in the 0.3  $\mu\text{m}$  channel, particles over 0.3  $\mu\text{m}$  to 0.5  $\mu\text{m}$  in size are represented in the 0.5  $\mu\text{m}$  channel, particles measuring over 0.5  $\mu\text{m}$  to 0.7  $\mu\text{m}$  are represented in the 0.7  $\mu\text{m}$  channel, particles over 0.7  $\mu\text{m}$  to 1.0  $\mu\text{m}$  are represented in the 1.0  $\mu\text{m}$  channel, particles over 1.0  $\mu\text{m}$  to 2.0  $\mu\text{m}$  in size are represented in the 2.0  $\mu\text{m}$  channel, and particles measuring over 2.0  $\mu\text{m}$  to 5.0  $\mu\text{m}$  are represented in the 5.0  $\mu\text{m}$  channel. The particle sampler's collection orifices are specifically engineered to disallow particles over 10  $\mu\text{m}$  from entering the counter.

For both particle samplers, particle size and counts are measured by passing incoming particles past a laser diode light. The particles displace the diode's projected light, which is focused on a photo diode by a set of collection optics. Each burst of displaced light is converted into an electrical pulse, the height of which is proportional to the particle's size (Figure 3.4). The pulse intensity is used to determine particle counts in particles/L.

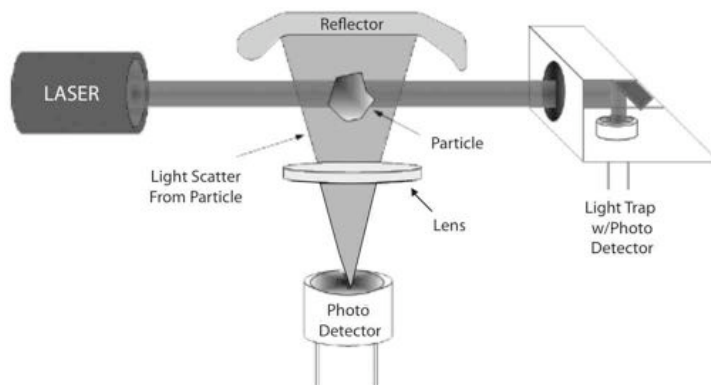


**Figure 3.4 – Schematic of a Laser Particle Counter's Optics (BPA, 2008)**

A shortcoming in the design of particle counters is that they assume a particle's shape to be spherical when calculating the particle's aerodynamic diameter. While a spherical shape is mostly true for small ( $<2.0 \mu\text{m}$ ) particles derived from high temperature emissions (anthropogenic) sources, larger particles sourced from re-entrained processes are likely to be jagged and uneven in shape (seen previously in Chapter 2, Figures 2.1 and 2.2).

Both particle counters were operated for one minute sampling period, with a set flow rate of 2.83 L/min. Multiple one-minute sampling runs were taken in sequence (usually three samples) and the counts were averaged. The counters were held at chest height, as this allows the counter to sample air at a height similar to breathing height. When used together, both the one-channel and six-channel sampler were run simultaneously. Sampled counts were recorded in a field book. The six-channel particle counter was calibrated by the manufacturer approximately three months prior the first set of sampling, and one year from the last set of sampling.

### **3.3 Particle Counting**

#### **3.3.1 Spatial Particle Counting**

The laser particle counters, because of their small size and ease of operation, could be employed at a variety of different sampling locations. The six-channel particle counter was used to sample at 88 city locations, chosen to evenly represent a cross section of the city (Figure 3.5). A series of 88 counts were taken on January 15 to 17, 2007, and a subset of the initial sites (33 sites) were sampled again on June 19, 2007. The initial sample set was taken during the dry season, and the latter sample set was taken during the wet season. Travel to each site was by motorbike, and samples were taken along the side of the road. Sample locations were spaced approximately one kilometer apart along roadways. Denser sampling was done along three transects; two along city roads, and one in the city dump.

The motorbike was turned off during sampling, and care was taken to choose a sample site located away from immediate combustion sources, such as street-side cooking with charcoal operating electrical generators, or other immediate sources, likely to provide elevated readings. The sampling methodology does skew the city particle counts to reflect conditions near roadways. However, many of the city's shops are located adjacent and are open to the street, or very close to it. Similarly most homes in Phnom Penh are also at street level, so correspondingly, most citizens are exposed to street level pollution for the majority of the day.

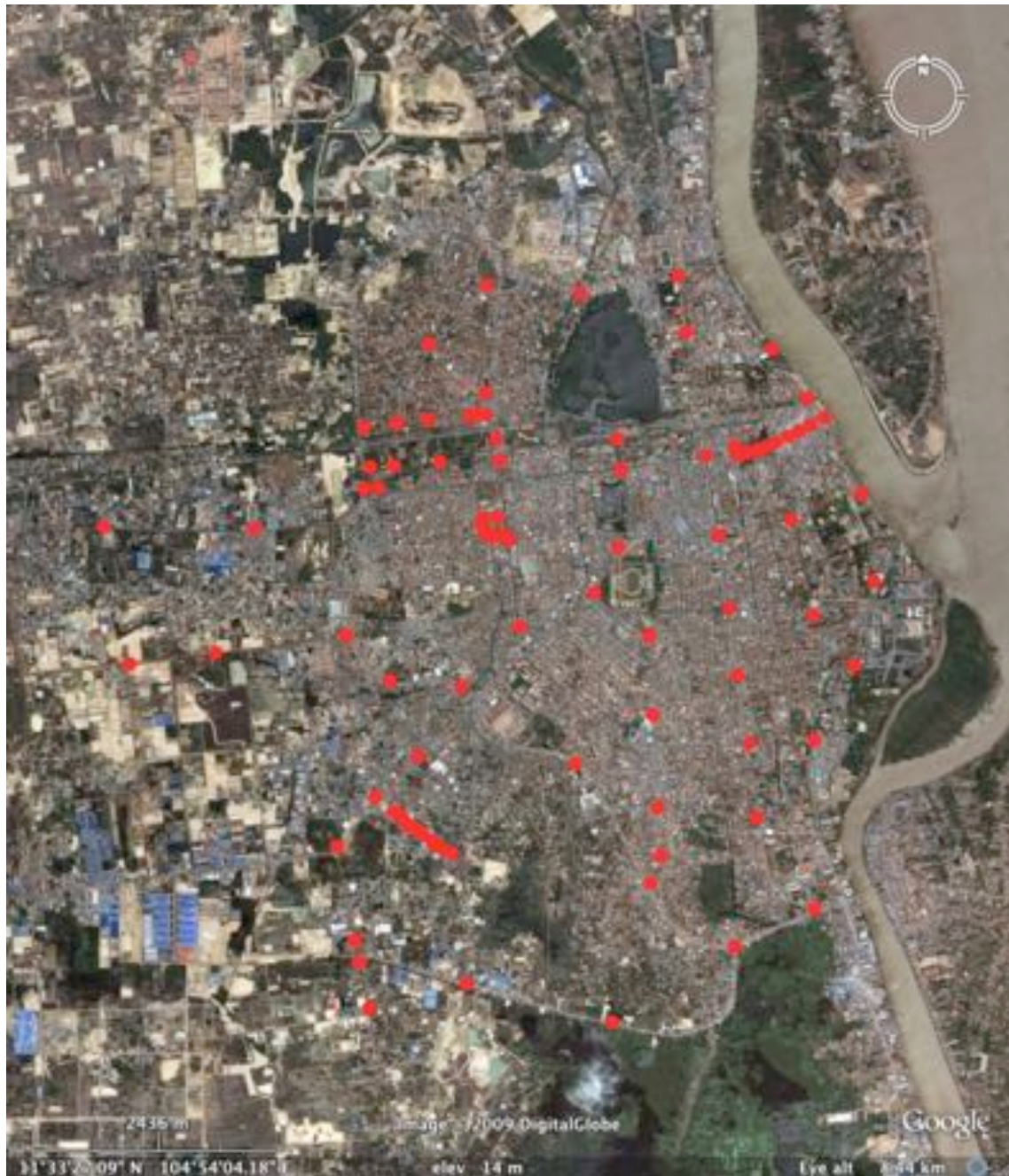


Figure 3.5 – 88 Spatial Particle Sampling Sites

### 3.3.2 Temporal Particle Sampling

Temporal analyses (daily profiles) were obtained using both the one and six-channel particle samplers at six locations that were chosen to represent typical Phnom Penh street and intersection traffic. Each sample location is plotted in Figure 3.6

As with the spatial sampling, sampling was again done at chest-height to represent the height at which a person draws air for respiration. Samplers were run for one-minute intervals at each sampling time throughout the day, with subsequent samples taken every half-hour.

Each location chosen for particle counting represents a different urban scenario. Locations were also chosen to obtain an approximate even distribution across the city. Because of the high cost and impracticality of bringing multiple samplers to Cambodia, along with the difficulty of securing more samplers once inside the country, the same particle samplers were used at each location, thus each location represents one unique day of sampling. While round-the-clock measurements of atmospheric particulates at each station would have been ideal, sampling times were constrained by limited personnel and equipment. Due to travel, equipment and personal safety issues, locations were sampled only during daylight hours with the exception of additional evening measurements taken at the Monivong Boulevard Comfort Star Hotel location.

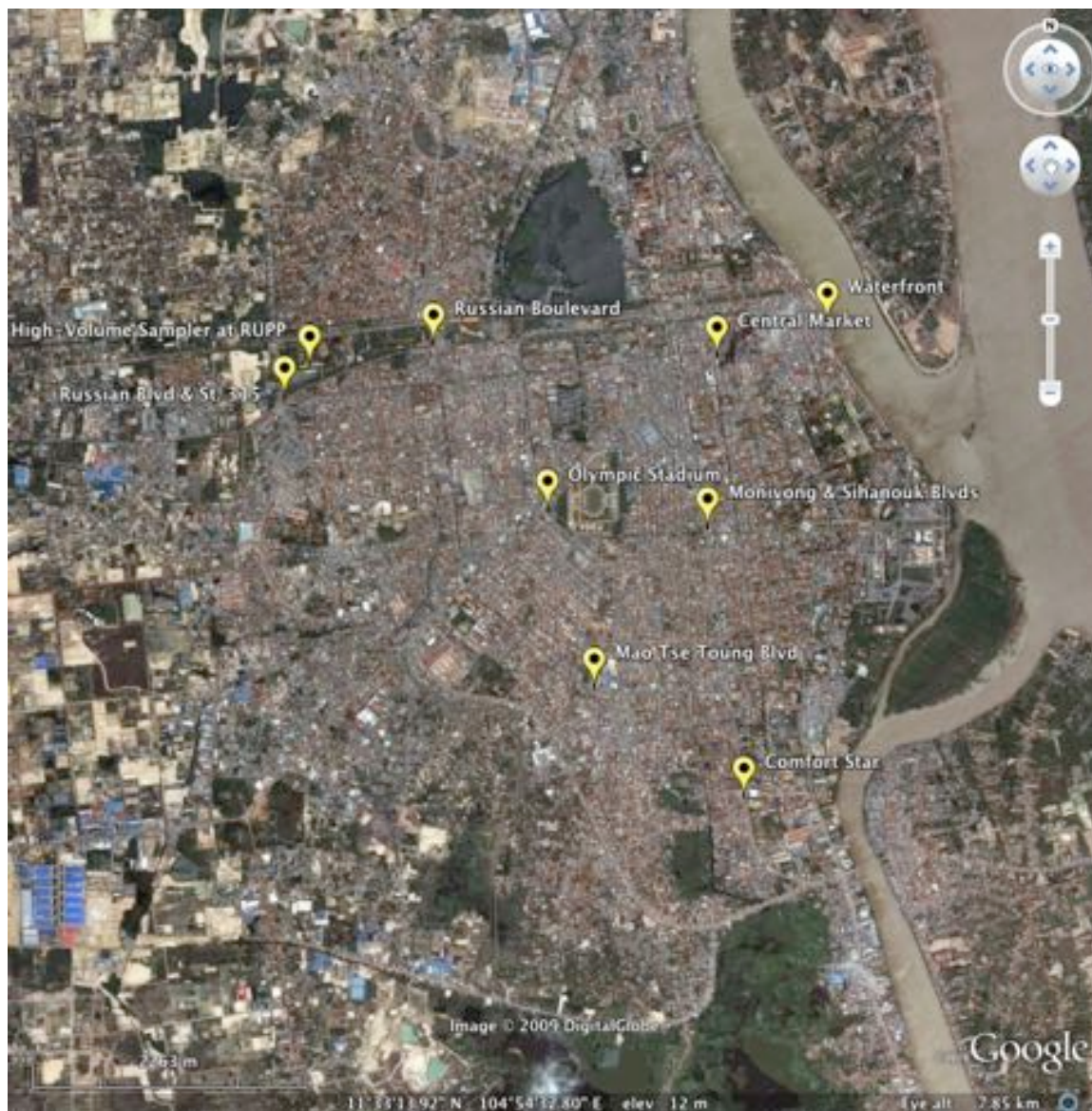


**Figure 3.6 – Temporal Sampling Sites in Phnom Penh**

**a. Comfort Star**

A location on the south end of Monivong Boulevard, at the Comfort Star Hotel, was chosen as a site to record temporal particle counts. Counts were recorded at this location on June 15, 2008 from 0500 to 1900 hours, June 20, 2008 from 1700 to 1900 hours, June 23, 2008 from 1800 to 2000 hours and June 23 from 1500 to 1930 hours. Monivong Boulevard is a major thoroughfare in Phnom Penh. The Comfort Star Hotel,

located near the Monivong Bridge over the Bassac River, represents an arterial road that conducts the flow of commuters into and out of the city.

**b. Russian Boulevard**

The Russian Boulevard sampling location represents an arterial road that carries traffic East to West into and out of the city from the airport and the surrounding countryside. Particle counts were recorded at this location on June 17, 2008 from 0900 to 1600 hours.

**c. Monivong and Sihanouk Boulevard**

The location at the intersection of Monivong and Sihanouk Boulevards represents a major intersection in the inner-city business district in Phnom Penh. Particle counts were recorded at this location on June 19, 2008 from 0900 to 1600 hours. Traffic flows in equal amounts North and South down Monivong Boulevard from the Central Market as it does East and West along Sihanouk Boulevard from the Olympic Stadium to the Waterfront.

**d. Central Market**

The Central Market sampling location represents a busy inner-city district and is one of the busiest locations in Phnom Penh. Particle counts were recorded at this location on June 20, 2008 from 0900 to 1600 hours on each hour interval (0900, 1000, 1100 etc.). A constant flow of traffic around the central market along with ever-present crowds and business generates large amounts of emissions.

**e. Waterfront**

The waterfront sampling location represents a commercial district with heavy traffic on the Northwestern edge of Phnom Penh, along the Tonle Sap River. Particle

counts were recorded at this location on June 20, 2008 from 0930 to 1530 hours on each half-hour interval (0930, 1030, 1130 etc.). Like the lower Monivong Boulevard location, this sample site incorporates business, and residential emissions, as well as commuting traffic entering or leaving the city on an arterial road.

**f. Mao Tse Toung Boulevard**

The Mao Tse Toung Boulevard location represents an inner-city intersection as is situated on a major east/west thoroughfare in an area in central Phnom Penh surrounded by business and residential buildings. Particle counts were recorded at this location on June 21, 2008 from 0900 to 1600 hours.

**g. Olympic Stadium**

The Olympic Stadium sampling location represents an inner-city environment composed of mixed-use business and residential buildings. Particle counts were recorded at this location on June 22, 2008 from 0900 to 1930 hours. Thoroughfare roads surround the stadium on three of four sides. The sample site was located at a four-way intersection between Monireth, Jawaharlal Nehru, Sihanouk, and Charles De Gaulle Boulevards.

**h. Russian Blvd & Street 315**

The sampling site located on the eastern edge of the Russian Boulevard at an intersection to the west of the Royal University of Phnom Penh represents a location on an arterial road that shuttles commuting traffic into and out of the city. This location was also chosen due to its close vicinity to the high-volume sampler located at RUPP. Particle counts were recorded at this location on June 24, 2008 from 0900 to 1530 hours.

### 3.3.3 Rural Particle Samples

Rural particle samples were taken on June 18, 2008 in Kean Svay district using the one-channel particle counter. Ten samples were collected on or near dirt roads that serve only local village traffic. At each location, three subsequent one-minute samples were taken for quality control purposes. Rural samples were collected to characterize a normal background level of particulate concentrations in a rural area with limited traffic and industry.

### 3.3.4 Bangkok Particle Samples

Particle counts were also collected during the wet season in Bangkok, Thailand on June 14, 2008. Counts were taken using the one-channel laser particle sampler. Particle counts were taken at street level underneath each Bangkok Mass Transit Skytrain station (n=23) in downtown Bangkok, so that a general cross section of the city was measured.

### 3.3.5 Analytical Methods

Counts taken with the laser particle counters were taken in one-minute intervals with a nominal flow rate of 2.83L/min (0.00283 m<sup>3</sup>/min). Values discussed in this study are presented as particles per cubic meter (particles/m<sup>3</sup>), converted by the following formula:

$$\text{Particles}/m^3 = \text{Particles}/2.83L \times 1000 \times 2.83$$

Because of the large number resulting from this conversion, numbers are reported in scientific notation.

Temporal particle count concentrations were graphed using Microsoft Excel software. Raw counts were graphed for each sample site. A two period moving average trend line was added to a graph if particle counts for that particular site had large and somewhat aggressive variations between subsequent half-hour increment samples. A three period moving average trend line was added if variations between each sample were very rapid and aggressive. A moving average trend line simply takes the average of a desired number of points (two, three, four etc... period), averages the point's data and plots the average on a graph. When a moving average trend line is used, it shifts the trend line down the x-axis in respect to the period selected, for example, a trend line will shift one slot down the x-axis if a two period trend line is used, or two slots down the x-axis if a three period trend line is used. The sole purpose of a moving average trend line is that it smoothes out variations in graphed data, allowing a reader to better understand trends portrayed in the graph.

The data analysis tool pack in Microsoft Excel was used on the raw data for each location to produce descriptive statistics (mean, median and standard deviation) for recorded particle count concentrations. To provide a visualization of temporal particle patterns rather than counts, a simple normalization was done on the data sets. Data was normalized by dividing an individual particle count at the site in question, by the mean particle count for all temporal samples taken at that same site. The resulting data produces a normalized data set disregarding the actual particle count so that different size fractions or sample sites can be directly compared.

### 3.4 High-Volume Air Sampler

A portable high-volume air sampler (Science Source Air Sampler #15000) was used to sample airborne ambient particulates. The high volume sampler was located at a single location on the grounds of the Royal University of Phnom Penh (RUPP). The sampler used in this study was chosen because of its small size and ease of portability, measuring only 40 cm in height. As with other high-volume samplers, the Science Source Air Sampler uses a motor to draw in air through an orifice and out through an exhaust escape (see Figure 3.7). The sampler operates at an estimated average flow rate of between 650 and 700 L/min, nominally set at 650 L/min. The flow rate is expected to decrease as the filter becomes loaded with collected particulates.



**Figure 3.7 – Photograph of the Portable High Volume Air Sampler**

The sampler's intake orifice is covered with a metal mesh, allowing a filter to be placed upon it to trap airborne ambient particles. The filter used in this study was a six-inch diameter quartz fiber filter, as provided by the sampler's manufacturer. The

placement of a white plastic ring around the filter keeps the filter in place, and forces air to pass only through the filter. Over the intake, a small plastic covering protects the filter from precipitation. To operate, the sampler must be secured on a flat surface.

The high-volume sampler was stationed on the second floor of RUPP (see Figure 3.8 for a close-up photograph of the high volume sampler, and Figure and 3.9 for a photograph of the sampler in situ at RUPP), and was configured to run an average of six hours, from approximately 0800 to 1600 hours. Some variation exists in the sampling time due to power outages in Phnom Penh. The sampler's location, on the second level of RUPP, does not provide a street level sample and is located approximately 130 meters from a major roadway. Care had to be taken to ensure a power source, the sampler's unsupervised security and continued operation.

The one-channel laser particle counter was employed to sample the air directly above the high volume sampler immediately before and after the high volume sampler was run so that recorded particle counts could be compared to particle mass loadings as collected by the high-volume sampler.



**Figure 3.8 – Close-up Photograph of the Portable High Volume Sampler at RUPP**



**Figure 3.9 – Photograph of the Portable High Volume Sampler in situ at RUPP**

### **3.4.1 Analytical Methods**

After the sampling period was complete, the high-volume was powered off, and the filter removed. The exposed side of the filter was then folded in half so that loss of the entrained particles is minimized. Each filter was sealed and labeled individually in an envelope to ensure that they remained uncontaminated. The quartz fiber filters used in the high volume air sampler were desiccated for twenty-four hours before the tare weight was taken (Cole-Parmer Symmetry Balance, accurate to 0.0001 grams), and again after the filters were loaded. The filter mass, recorded in grams, was converted to

concentration ( $\mu\text{g}/\text{m}^3$ ) by subtracting the filter's previously recorded tare weight from the loaded filter's mass. The resulting difference is then divided by the sampling time in minutes multiplied by the average flow rate in liters per minute. The following formula can be derived in order to calculate the concentration (c) in grams per liter (g/L):

$$C_{g/L} = \frac{M_L - M_T}{(t \times Q)}$$

where:

$M_L$	=	mass of the loaded filter
$M_T$	=	filter tare weight
$t$	=	sampling time in minutes
$Q$	=	average flow rate

The resulting concentration (c) in g/L can be converted to  $\mu\text{g}/\text{m}^3$  by dividing the concentration in grams per liter by  $1 \times 10^{-9}$  or using the formula:

$$C_{\mu\text{g}/\text{m}^3} = \frac{C_{g/L}}{.000000001}$$

Particle mass loadings were graphed on a scatter plot in Microsoft Excel along with average particle number counts as recorded with the laser particle counter. A linear regression trend was superimposed on the scatter plot to display the positive correlation between the two parameters. A two-tailed t-test was performed with a significance level of 0.05 to distinguish that the trend is significantly different than zero.

### **3.5 Surface Dust/Dirt Samples and Bulk Deposition Analysis**

#### **3.5.1 Surface Dust/Dirt Samples**

Surface dust samples were collected from six urban sites and four rural sites to apportion the particles measured by the high volume air sampler to general source areas (e.g. urban or rural) using X-ray fluorescence (XRF). Surface dust/dirt samples were collected with the use of a sterilized horsehair brush. Urban street samples of approximately 10 grams in mass were swept directly from the side of paved streets into a polyethylene bag. Rural samples were taken from dirt roads and fields by again sweeping approximately 10 grams of dust into a polyethylene bag using a constant sweeping motion with the horsehair brush. The bags were labeled and sealed until an analysis could be performed.

#### **3.5.2 Bulk Deposition Analysis**

Bulk deposition were samples collected weekly from July 6 to September 28, 2008 at four residential locations in Phnom Penh. Samples were collected using plastic buckets with an orifice of approximately 12 inches. After the sampling period, the collectors were removed, and the accumulated deposited material was rinsed out and filtered through pre weighed filters using a vacuum hand pump filter. The filters were then sealed in an envelope until analysis with XRF was performed.

#### **3.5.3 Elemental Composition Analysis**

Elemental compositions of the particles collected in the road dust grab samples and bulk deposition samples were analyzed using a Thermo Scientific Niton XLt Field Portable X-ray Fluorescence (FPXRF) unit at SUNY Buffalo State College. The FPXRF unit is equipped with a low power (1.0 W) Ag anode x-ray tube and a Si PiN detector,

and was run for a sampling time of 120 seconds in bulk soil mode (Thermo Scientific, 2007).

FPXRF units are deployed because of their relative ease of use, and extremely fast, high quality results in the field with minimal sample preparation (Bernick, et al., 1995). FPXRF analyzers, while convenient for field use, have higher level of detection limits for fewer amounts of elements than laboratory-strength models, especially with elements with a lighter mass.

Most XRF units use energy dispersive analyzers that convert the X-ray's detective properties into an electronic pulse based on photon energy. The FPXRF used (Niton XLt) employs the use of an x-ray tube that irradiates samples, exciting the sample's electrons. X-rays knock electrons out of the inner shells. Electrons then move from the outer shells to move into the inner orbits to fill the vacancies. When electrons fall into inner orbits to fill vacancies, they emit a pulse of energy, equivalent to the energy difference between the two electron shells in question (Bergslien, personal communication, 7 Nov. 2008). A general diagram of electron behavior when acted upon by an x-ray from a FPXRF unit is shown in Figure 3.10.

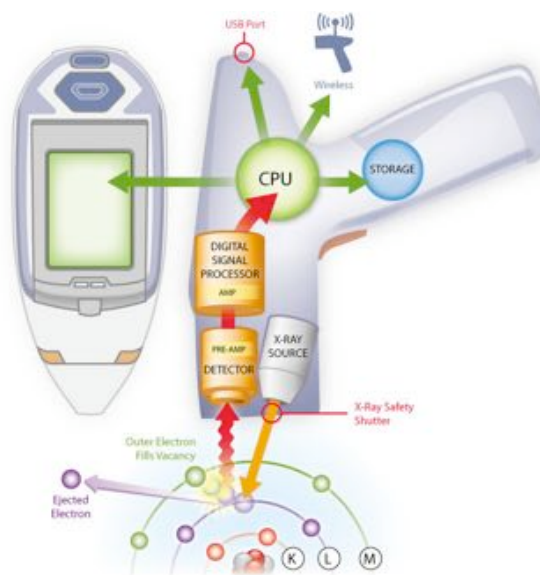


**Figure 3.10 – Diagram of Electron Behavior During XRF analysis (Niton, 2008)**

Road dust samples were prepared for FPXRF analysis by placing them in an XRF sampler holder covered with a 2.5  $\mu\text{m}$  thick mylar film. The FPXRF was operated using a bench top mount and was set to analyze each sample in a two-minute period. Bulk collection filters were placed on top of a Plexiglas plate and analyzed with the FPXRF used as a gun. By placing the filters on the Plexiglas plate, the FPXRF records only materials on top of the plate, and not the surface beneath it.

For quality control purposes, the FPXRF unit was calibrated prior to use as according to the manufacturer's specifications. Also, to ensure quality, each sample was run three times non-consecutively, interspersed with known standards.

The FPXRF unit provides results in two forms. The first is a spectral image of the energy given off by electrons as they move around the element's shells. A spectral image for the road dust sample collected at the Monivong Boulevard location is shown in Figure 3.11.

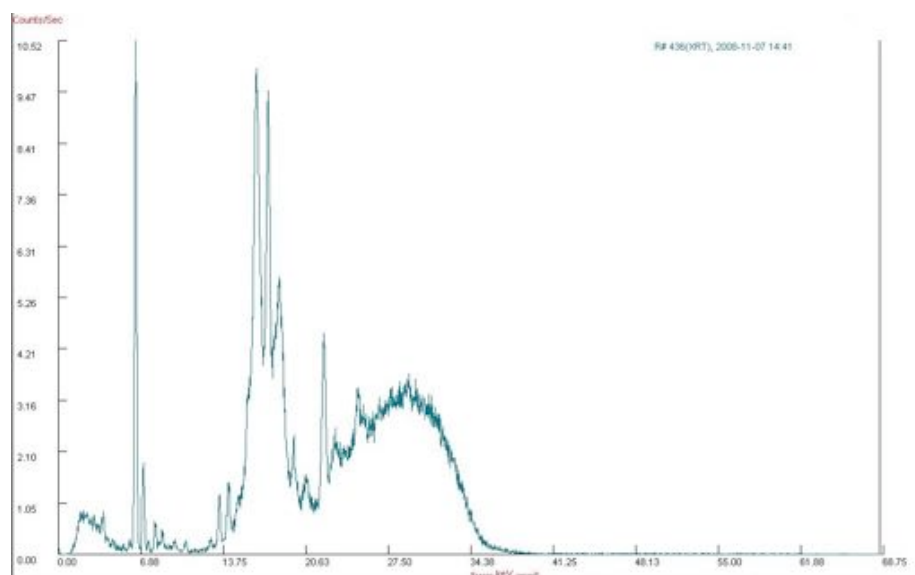


**Figure 3.11 – Spectral Image for Monivong Boulevard Comfort Star Hotel Road Dust Sample**

The spectral image displays the electron volts (keV) recorded by the XRF unit as energy is released when electrons change shells. The spikes shown in counts/sec show the frequency of electron loss, and are proportional to the amount of that particular element in the sample. Each element's electron has a unique keV energy, allowing for identification of the element in question. The gradual arch shown in Figure 3.11 from approximately 24 keV to 37 keV displays the properties of the detection of an unidentifiable amorphous matter.

The second result provided by the FPXRF is a spreadsheet file containing the concentrations (ppm) of each element recorded by the unit. For this study, the spreadsheet was imported into Microsoft Excel software for analysis using descriptive statistics.

### **3.5.4 Enrichment Factors**

Enrichment factors are a calculation used in many studies to determine if an element of interest is elevated above natural background levels suggesting an

anthropogenic source. Natural sources of particulates include crustal weathering and seawater. Reference material may range from rural dust samples, as these may represent a natural background level that is not heavily enriched by anthropogenic means, or global soil elemental composition averages as listed in the literature. EF values are calculated with the following formula:

$$EF = \frac{(C/R) \text{ road dust}}{(C/R) \text{ reference material}}$$

where: C = concentration of the element of interest  
R = concentration of the reference element

By comparing an element of interest to a known concentration of a background element, a ratio is calculated showing the level of abundance of the element of interest in relation to the reference element. An enrichment factor (EF) of 10 or higher is considered enriched, while an EF around 1 suggests the reference material as a source. Enrichment factors were calculated two ways for this study. First, averages of elemental composition for all urban and rural sites were produced, respectively. Then EF values were calculated using the rural material as the background level to determine whether the urban material is enriched. Second, EF values were calculated using the urban material as a reference to determine whether the bulk deposition material was enriched.

## Chapter 4 – Results and Discussion

### 4.1 Spatial Particulate Characteristics

#### 4.1.1 Dry Season Particulate Characteristics

Particle counts were taken in the dry season from January 15 to 17, 2007 with the six-channel laser particle counter. The median count for the 88 sample sites in Phnom Penh was  $1.07 \times 10^8$  particles/m<sup>3</sup> for fine fraction particles and  $1.36 \times 10^6$  particles/m<sup>3</sup> for coarse fraction particulates. As can be seen in Figure 4.26, fine particles were recorded in high concentrations throughout the city, and most notably in areas linked with high amount of traffic flow including major arterial roads and intersections. Lower counts of fine particles are seen around the waterfront, dirt roads, and other areas with a lower volume of traffic such as roads near the west and southwest edge of the city. Area A shown in Figure 4.26 represents a two-block perimeter that particles counts were taken on at multiple locations. Fine particle counts are fairly low in this area, likely due to its removal from immediate major roads, and the fact that some connecting roads were unpaved.

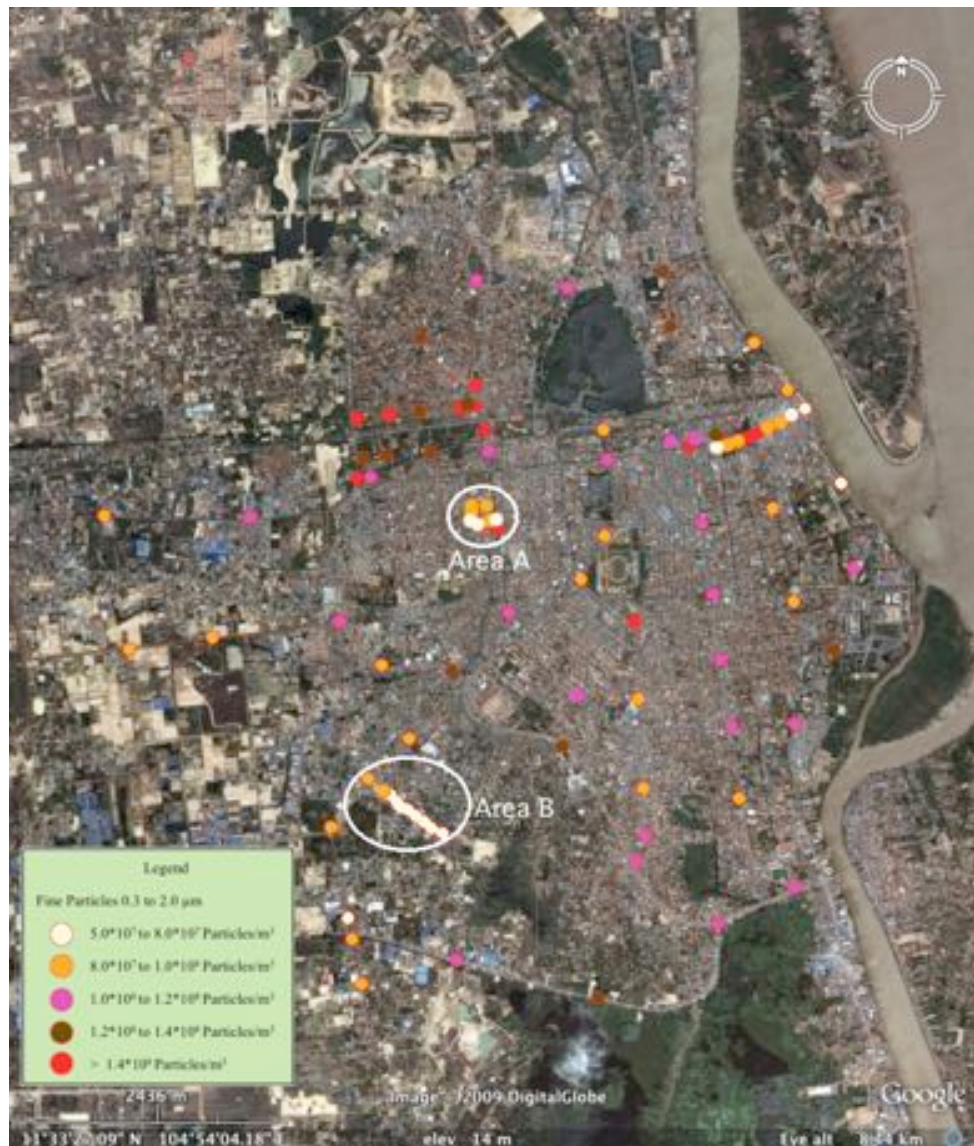


**Figure 4.1 – Fine Particulates in Phnom Penh**

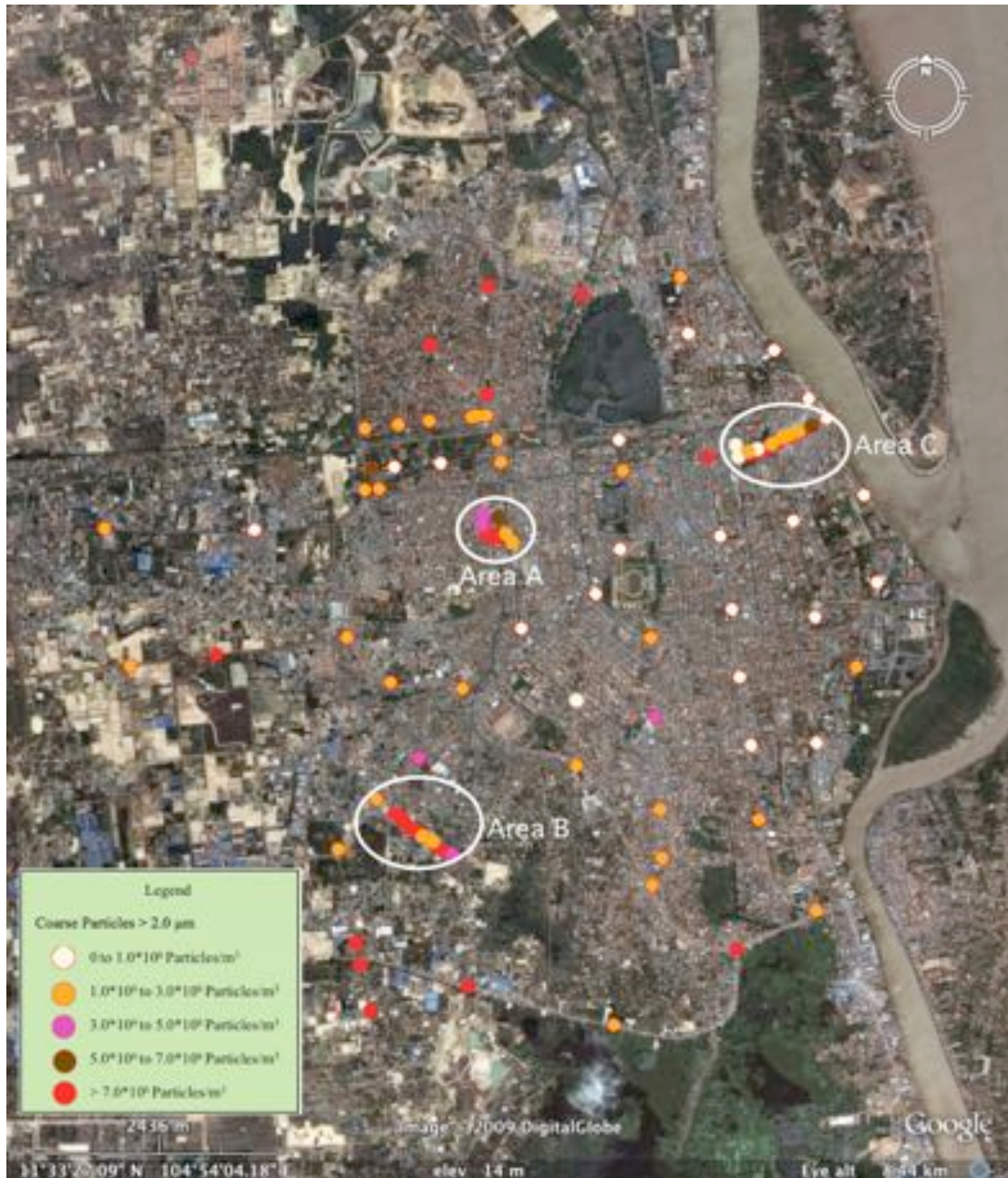
The garbage dump, seen in area B in Figure 4.1 shows lower than expected levels of fine particulates given the ever-present smoldering garbage encountered in the dump (photograph seen in Figure 4.2). The lower level of fine particulates in the dump is attributed to the fact that fine particulates are generally derived from high temperature combustion. The smoldering garbage is simply not high enough a temperature to produce submicron particles.



**Figure 4.2 – Garbage Dump in Phnom Penh**

Coarse particle counts, as seen spatially in Figure 4.3 show a dataset skewed towards a large number of high counts. A few dusty sites (i.e. sample sites located on dirt roads) are considered to be the primary drive of the elevated coarse particle levels. A look at the median and mean counts ( $1.36 \times 10^6$  vs.  $2.95 \times 10^6$  particles/ $m^3$ ) shows that the mean is roughly two times greater than median, suggesting a number of hotspots around the city that contain elevated concentrations of coarse material.

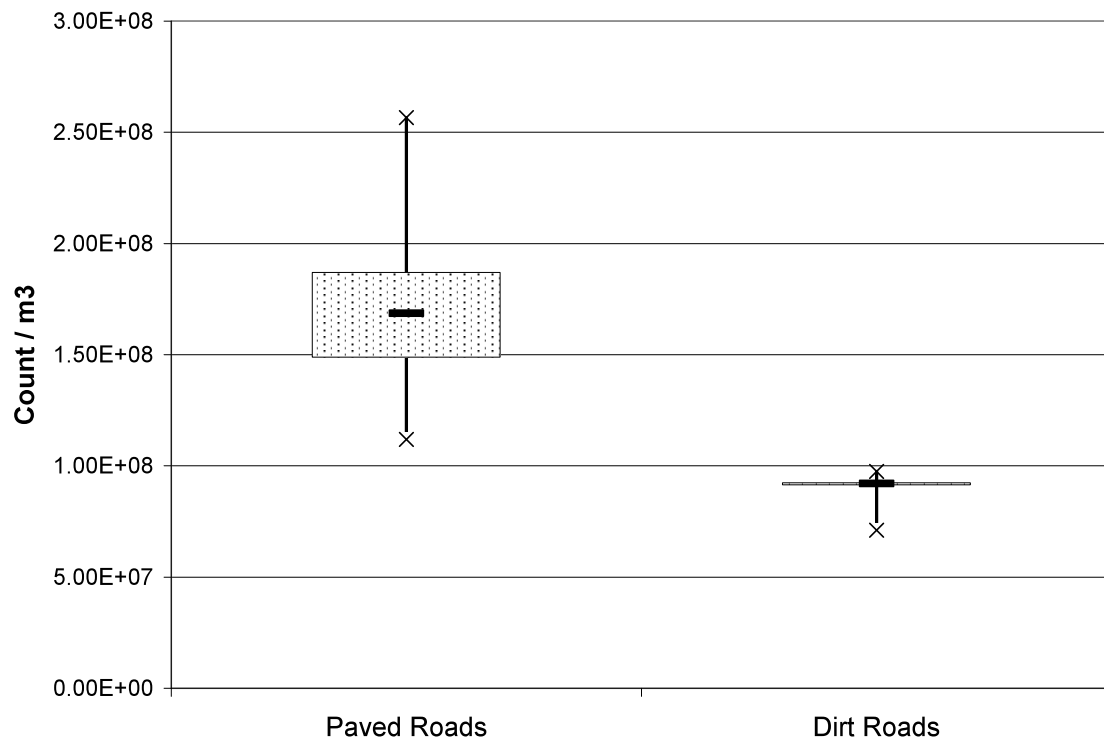
Mirroring the fine particles counts, the waterfront possesses the lowest concentration of coarse particles, a combination of the dilution effect by the river breezes as described in Furuuchi et al. (2006), and low numbers of unpaved roads. Areas A and B, a two-block perimeter and the garbage dump show levels of coarse particulates much higher than fine particulates in the same areas (Areas A and B in Figure 4.1). As shown by Area C in Figure 4.3, coarse particle counts generally fall off as sample sites get closer to the river, with the exception of one location registering high coarse particulate levels.



**Figure 4.3 – Coarse Particulates in Phnom Penh**

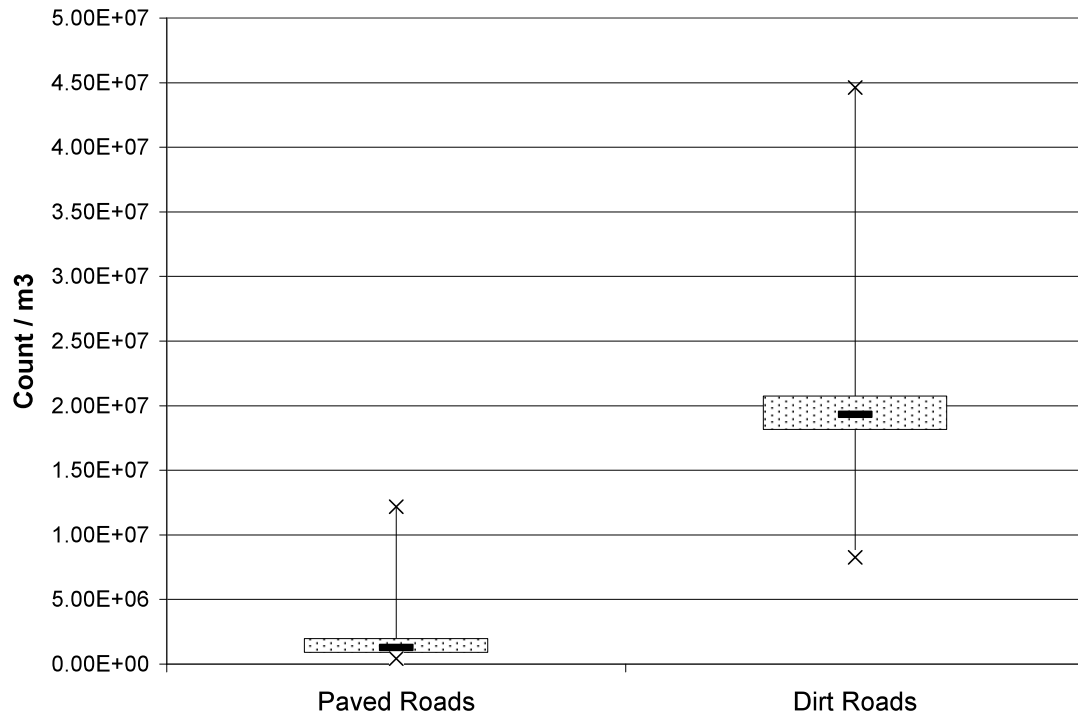
Particle counts recorded on paved roads had a median count of  $1.69 \times 10^8$  particles/m<sup>3</sup> while fine particles recorded on unpaved roads had a median count of  $9.21 \times 10^7$  particles/m<sup>3</sup>. This 46% difference suggests that paved roads have a higher concentration of fine particle-producing vehicular traffic than dirt roads.

Figure 4.4 shows the median count, along with the range and inter-quartile range of fine particles recorded on each road surface. Figure 4.4 also shows that paved roads have a higher (1.5 times) median count of fine particles than dirt roads.



**Figure 4.4 – Fine Particulates by Road Surface in Phnom Penh**

Particle counts recorded on dirt roads ( $1.93 \times 10^7$  particles/m<sup>3</sup>) had coarse particle counts 15 times higher than those recorded on paved roads ( $1.28 \times 10^6$  particles/m<sup>3</sup>), suggesting that dirt roads provide a large majority of re-suspended coarse particles. Figure 4.5 shows that dirt roads have a coarse particle count much higher than paved roads. Figure 4.5 also displays a much greater range than present on paved roads. This is attributed to the hotspots discussed earlier in which a few number of sample sites on dirt roads have a coarse count disproportionately higher than the rest.



**Figure 4.4 – Coarse Particulates by Road Surface in Phnom Penh**

#### 4.1.2 Rural Particle Counts

A set of set of rural province particle samples was taken in the dry season using the six-channel particle counter. The particle counts had a mean concentration of  $4.48 \times 10^8$  particles/m<sup>3</sup>, a median of  $2.95 \times 10^8$  particles/m<sup>3</sup>, and a standard deviation of  $4.68 \times 10^8$  particles/m<sup>3</sup>.

The mean particle count for the rural samples taken in the wet and dry seasons differ by only 1%, even though they were taken approximately a year apart from each other, showing that a constant mean particle count exists in rural areas and remains independent from seasonal fluctuations.

## 4.2 Wet vs. Dry Season Particulate Characterizations

A re-sampling of 33 out of 88 sample sites was conducted in the wet season on June 19, 2007 in order to gauge the seasonal spatial differences of particulates using the six-channel laser particle counter. Median fine particle counts dropped by 22%, while median coarse particle counts dropped by 37%. The mean fine particle count dropped by 14%, suggesting that seasonal variations play only a small role in fine particle counts when compared to coarse particle counts, which were shown to drop by 55% over the same two seasons. These data suggest that the 14% drop in fine particulates may be attributed to lower vehicle traffic in the rainy season, as fine particle concentrations dropped in across the board at many sites. Coarse particle concentrations were recorded at the same 33 sites in both the dry and wet seasons. Coarse particulates, by dropping 55%, suggest that the rainy season prevents much of the coarse material on dirt roads from being readily re-suspended as it does in the dry season, when the dirt roads are dry.

### 4.2.1 Wet Season Particulate Characteristics

Mean particle counts for all samples taken within Phnom Penh during the wet season in 2008 are  $6.85 \times 10^8$  particles/m<sup>3</sup> with a standard deviation of  $2.46 \times 10^8$  particles/m<sup>3</sup>. Median particle counts for the same period were  $6.33 \times 10^8$  particles/m<sup>3</sup>.

Particle Counts taken at ten rural sites southeast of Phnom Penh had a mean count of  $4.50 \times 10^8$  particles/m<sup>3</sup> with a standard deviation of  $6.92 \times 10^7$  particles/m<sup>3</sup> and a median particle count of  $4.35 \times 10^8$  particles/m<sup>3</sup>.

Figure 4.6 displays the mean particle count concentrations for each urban and rural site sampled in the wet season. Across the board, the urban sites recorded higher

levels of PM<sub>10</sub> than most of the rural sites, suggesting that the majority of the measured particulates in Cambodia are from anthropogenic sources, and concentrated in the smaller size fractions of particulate matter.

For the rural sites, each location has a similar recorded particle count concentration, but it can be seen that the sixth consecutive sample had particle counts elevated from the other samples. The reason for this is that at the time of the sampling, a nearby house was engaged in cooking on a grill with wood biofuel. Because of the nature of cooking with biofuels, it is suggested that the elevated particle count shown in Figure 4.6 is comprised of a larger number fine fraction particulates than the other sample sites. Figure 4.6, along with the standard deviations of  $2.46 \times 10^8$  and  $6.92 \times 10^7$  particles/m<sup>3</sup> for urban and rural site respectively, also suggest that urban particulate concentrations are a function of anthropogenic activity, while rural particulate concentrations tend to be more stagnant, and represent a baseline count, or natural background level.

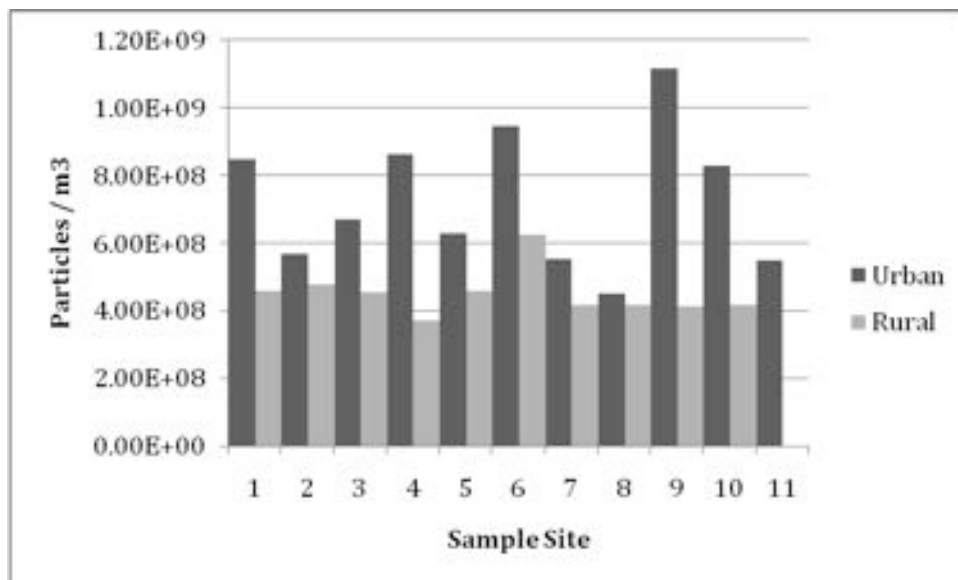


Figure 4.6 – Mean Particle Counts for PM<sub>10</sub> at Sample Sites at Urban and Rural Sites

Particle counts for both urban and rural locations are aggregated into Table 4.1 for analysis. Particle counts taken in the rural province were 66% lower than those taken in Phnom Penh. The difference was confirmed by a t-test. This shows that particulates are more abundant in urban areas. The fact that urban areas contain more exhaust-producing vehicles than the countryside helps to certify this assertion.

**Table 4.1 – Particle Counts for PM<sub>10</sub> at Sample Area in Urban and Rural Phnom Penh**

<i>Sample Areas</i>	<i>Mean Particle Count (particles/m<sup>3</sup>)</i>	<i>Median Particle Count (particles/m<sup>3</sup>)</i>	<i>Standard Deviation</i>
Urban Phnom Penh	6.85*10 <sup>8</sup>	6.33*10 <sup>8</sup>	2.46*10 <sup>8</sup>
Rural Phnom Penh	4.50*10 <sup>8</sup>	4.35*10 <sup>8</sup>	6.92*10 <sup>7</sup>

It is expected that fine particle concentrations will be elevated in urban areas due to the larger number of operating vehicles and other combustion sources than in rural areas. While the fine fraction particulates from exhaust may account for the large majority of particles, it is also possible that because vehicles are more abundant in urban areas, they also contribute to the re-suspension of coarse material. A field in a rural area may be covered with coarse material, but that material will only be re-suspended by natural processes like wind, while in an urban environment, coarse material may be re-suspended by both natural and anthropogenic processes. This however does not mean that cities have more suspended coarse particles. The overall dearth of vehicles in rural areas means that less fine fraction particles are in the ambient air. Other anthropogenic activities like cooking and burning of biofuels contribute fine particles in rural environments.

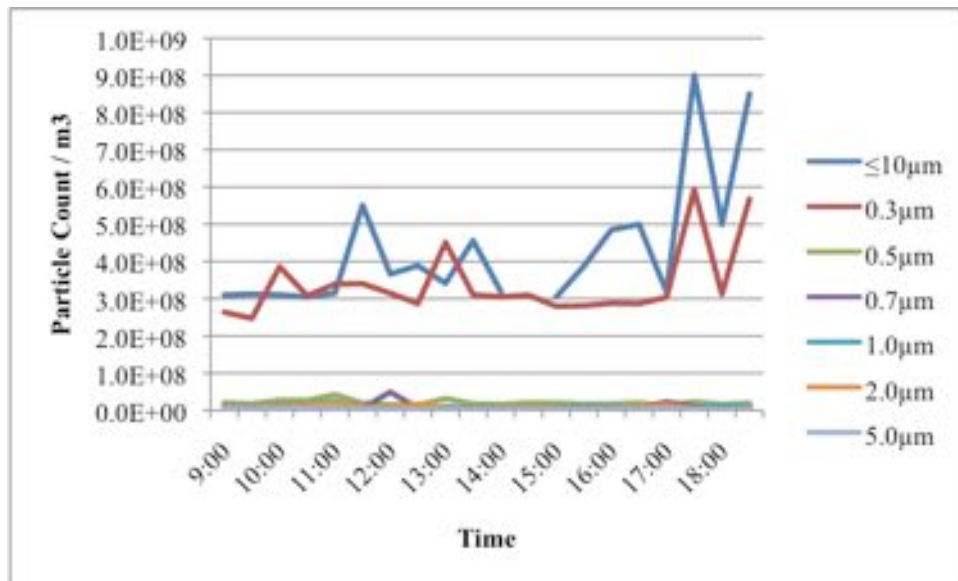
The mean particle count in Bangkok was  $6.16 \times 10^8$  particles/m<sup>3</sup>. The median count was  $5.95 \times 10^8$  particles/m<sup>3</sup> and the standard deviation was  $2.19 \times 10^8$  particles/m<sup>3</sup>. The median particle count in Phnom Penh was 106% higher than the median particle count in Bangkok during the wet season. Particle counts in Bangkok had a lower coefficient of variation than Phnom Penh (0.35 vs. 0.36) and a lower (by 11%) standard deviation than samples taken in Phnom Penh. These show that particulate levels in Bangkok are more consistent than those in Phnom Penh, because the city has a more homologous urban environment including building type and arrangement and traffic density and patterns.

#### 4.2.2 Size Fraction Contributions

It is necessary to understand the percent contribution of each particle size to each particle count taken. For this study, the six-channel particle counter was used only three times at two unique sites. Using the limited data available from this particle counter, it is proposed that each group of particle sizes fall within a predictable range of percent contribution. Particles sized 0.3, 0.5, 0.7, 1.0, 2.0 and 5.0  $\mu\text{m}$  had a percent contribution of 85, 9.8, 4.0, 3.4, 1.6 and 0.3% respectively. This shows that as expected, smaller particles contribute most to the count of ambient particulates, while larger particles contribute the least.

Figure 4.7 displays raw data particle counts for both  $\leq 10 \mu\text{m}$  and 0.3-5.0  $\mu\text{m}$  size groupings at the Olympic Stadium location in central Phnom Penh on June 22, 2008. A gap due to missing data at the 1330 hours sample for particle  $\leq 10 \mu\text{m}$  is also shown. It is clear that the majority of the particles measured by the six-channel particle counter reside in the 0.3  $\mu\text{m}$  fraction. The 0.3  $\mu\text{m}$  size fraction approaches and

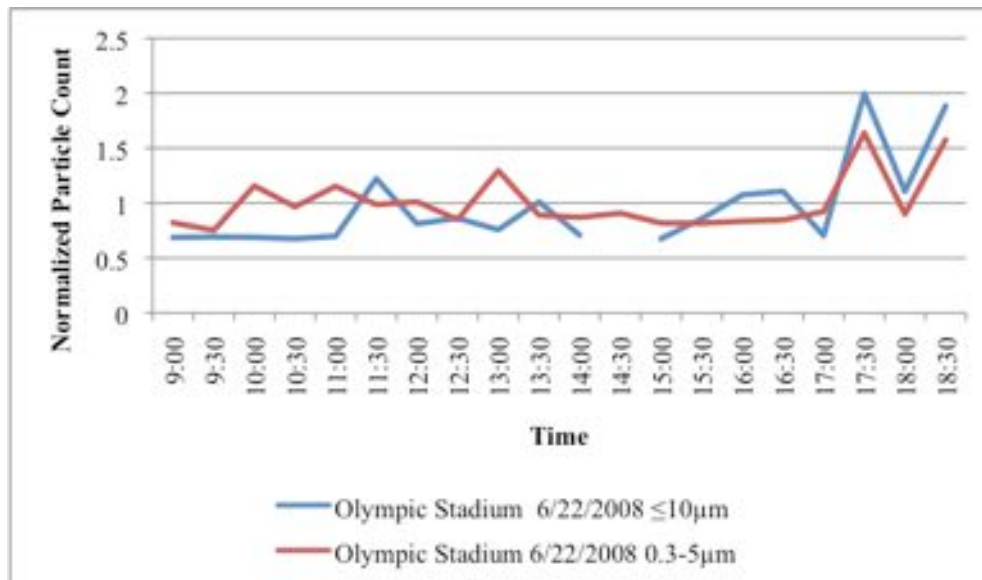
occasionally surpasses the level of  $PM_{10}$ , while the 0.5-5.0  $\mu m$  size fractions cluster together in lower concentrations.



**Figure 4.7 – Temporal Particle Counts for Particles  $\leq 10\mu m$  and 0.3-5.0  $\mu m$  at Olympic Stadium**

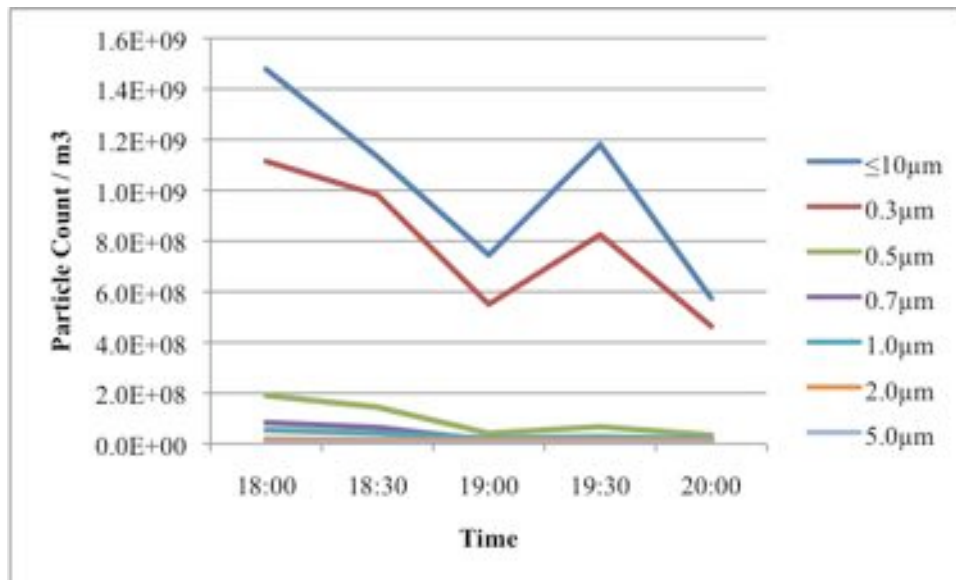
**Location on June 22, 2008**

A graph using calculated normalized values for particles  $\leq 10\mu m$  and 0.3-5.0  $\mu m$  (Figure 4.8) shows that, while several spikes in either fraction's concentrations were recorded, the two size groupings match with a general correspondence, and never differed by more than a factor of two.



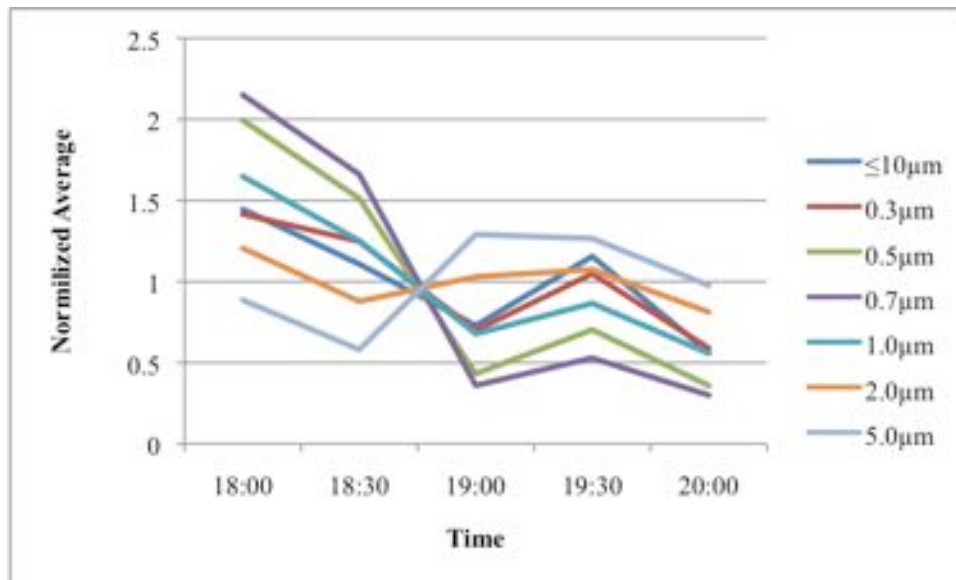
**Figure 4.8 – Normalized Temporal Particle Counts Comparing Particles  $\leq 10 \mu\text{m}$  and  $0.3\text{-}5.0 \mu\text{m}$  on June 22, 2008 at the Olympic Stadium Location**

Evening PM measurements recorded at the Comfort Star location on June 22, 2008, show  $\text{PM}_{10}$  and  $\text{PM}_{0.3-5.0}$  closely following each other with a 95% correlation. The downward trend shown in Figure 4.9 is representative of the decrease in particle counts seen across the board after the evening rush hour traffic disperses. As shown previously in Figure 4.7, a similar relationship exists between the  $\text{PM}_{10}$  and  $\text{PM}_{0.3-5.0}$  size groups. These two size fraction groupings are shown together again in Figure 4.9. Because of the similar concentrations of particles  $\leq 10 \mu\text{m}$  and particles sized  $0.3 \mu\text{m}$ , it is noted that the bulk of the measured particulates in  $\text{PM}_{10}$  in Phnom Penh are in the  $0.3 \mu\text{m}$  fraction, while  $0.5\text{-}5.0 \mu\text{m}$  make up the rest of the grouping clustered together in lower concentrations.



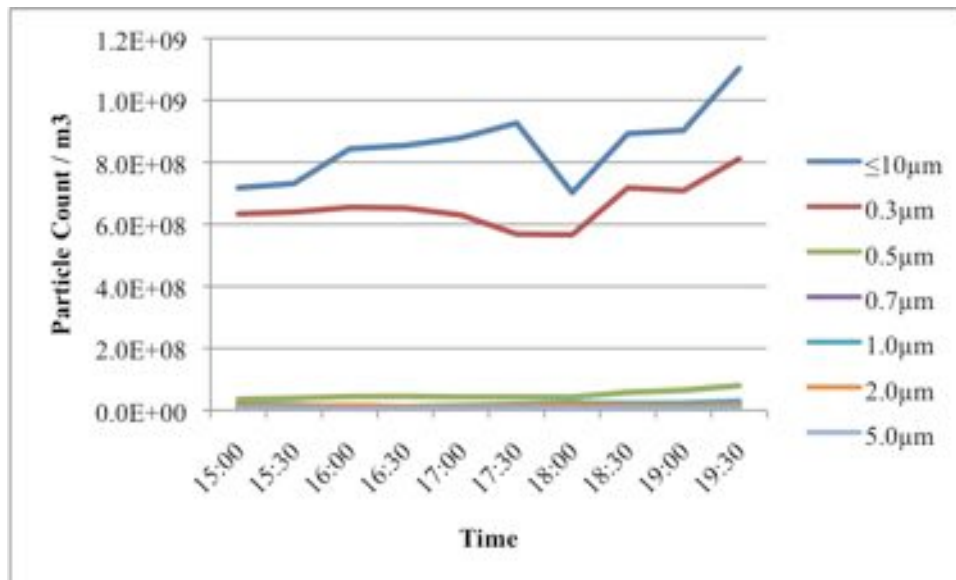
**Figure 4.9 – Temporal Particle Counts for Particles  $\leq 10 \mu\text{m}$  and  $0.3\text{--}5.0 \mu\text{m}$  at Monivong Boulevard Comfort Star Hotel Location on June 22, 2008**

Figure 4.10 displays normalized values for each size fraction, and it can be seen that every size fraction displays similar trends of starting high, decreasing until 1900 hours, and rising slightly from 1900 to 1930 hours before decreasing a last time until 2000 hours. The exception is the  $5.0 \mu\text{m}$  size fraction, and to a lesser extent the  $2.0 \mu\text{m}$  size fraction which sees a rise in particle concentrations from 1830 hours to 1900 hours, suggesting that something at this location causes coarse particle concentrations to rise during that sampling time.



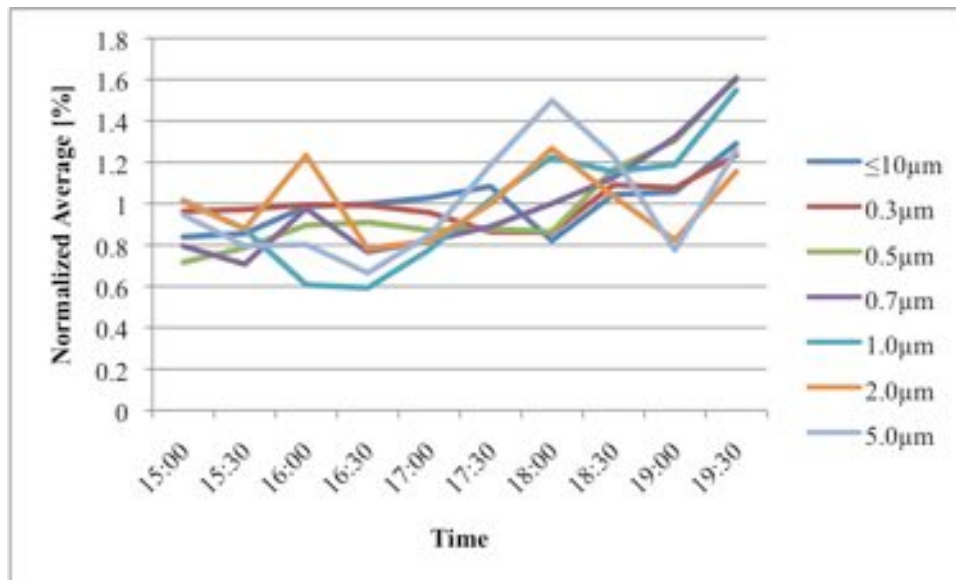
**Figure 4.10 – Normalized Temporal Particle Counts Comparing Particles  $\leq 10\ \mu\text{m}$  and  $0.3\text{-}5.0\ \mu\text{m}$  on June 22, 2008 at the Comfort Location**

Particle counts recorded at the same location on June 23, 2008, display a different particle concentration trend. Beginning at 1800 hours, where in previous measurements, a gradual decline in particulate concentrations is seen, levels sharply rise. Figure 4.11 displays this trend with both  $\text{PM}_{10}$  and  $\text{PM}_{0.3-5.0}$ . While the  $\text{PM}_{10}$  in the late afternoon and early evening hours are elevated, the two groups of particle sizes behave almost exactly beginning at 1800 hours. During the measurement period, the two parameters ( $\text{PM}_{10}$  and  $\text{PM}_{0.3-5.0}$ ) have a correlation of 74%, while the measured concentrations from 1800 to 1930 show a correlation of 97%.



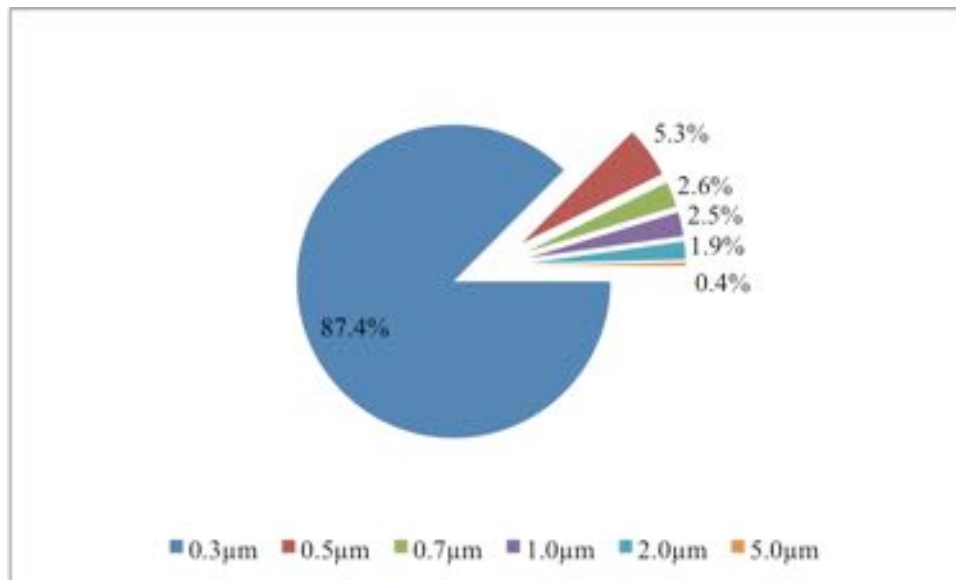
**Figure 4.11 – Temporal Particle Counts for Particles  $\leq 10 \mu\text{m}$  and  $0.3\text{-}5.0 \mu\text{m}$  at Monivong Boulevard Comfort Star Hotel Location on June 23, 2008**

Figure 4.12 displays the overall trends of particles for all measured size fractions at this location. While some variability in particle counts exists, the overall trend displayed shows that counts recorded at the end of the sampling period (1930 hours) are higher than counts recorded at the beginning of the sampling period (1500 hours).



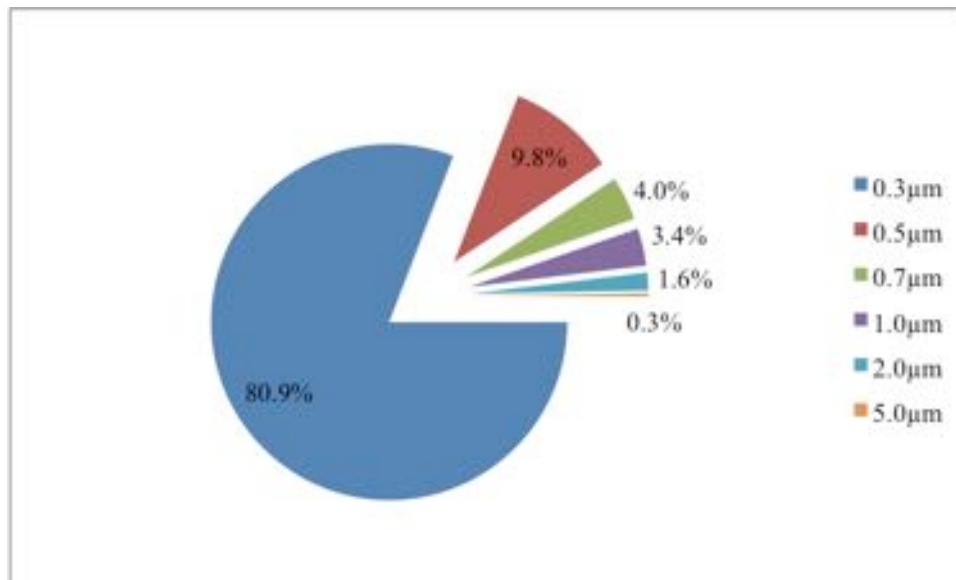
**Figure 4.12 – Normalized Temporal Particle Counts Comparing Particles  $\leq 10 \mu\text{m}$  and  $0.3\text{-}5.0 \mu\text{m}$  on June 23, 2008 Samples at the Comfort Location**

Percent contributions of particle counts for the Olympic Stadium location in central Phnom Penh on June 22 are seen in Figure 4.13. The  $0.3 \mu\text{m}$  size particles account for an average of 87.4% of the total recorded particulates at this location, while particles sized  $0.5 \mu\text{m}$  account for 5.3%, particles sized  $0.7 \mu\text{m}$  account and  $1.0 \mu\text{m}$  account for 2.6 and 2.5% respectively, particles sized  $2.0 \mu\text{m}$  account for 1.9% and particles sized  $5.0 \mu\text{m}$  account for 0.4% of the total recorded particles.



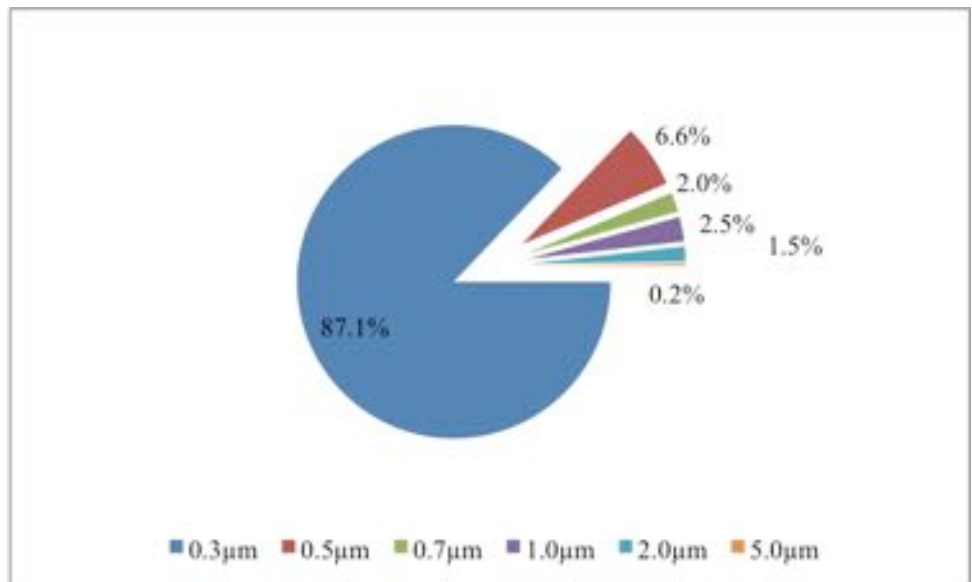
**Figure 4.13 – Average Percent Contributions for Particles sized 0.3-5.0 μm at the Olympic Stadium location on June 22, 2008.**

Percent contributions of each size fraction in the 0.3-5.0 μm grouping for the Monivong Boulevard Comfort Star Location on June 22, 2008 are shown in Figure 4.14. Particles sized 0.3 μm account for 80.9% of the total particle concentrations at this location, particles sized 0.5 μm account for 9.8%, particles sized 0.7 μm account for 4.0%, particles sized 0.1 μm account for 3.4%, particles sized 2.0 μm account for 1.6% and particles sized 5.0 μm account for 0.3% of the total particle concentrations at this location.



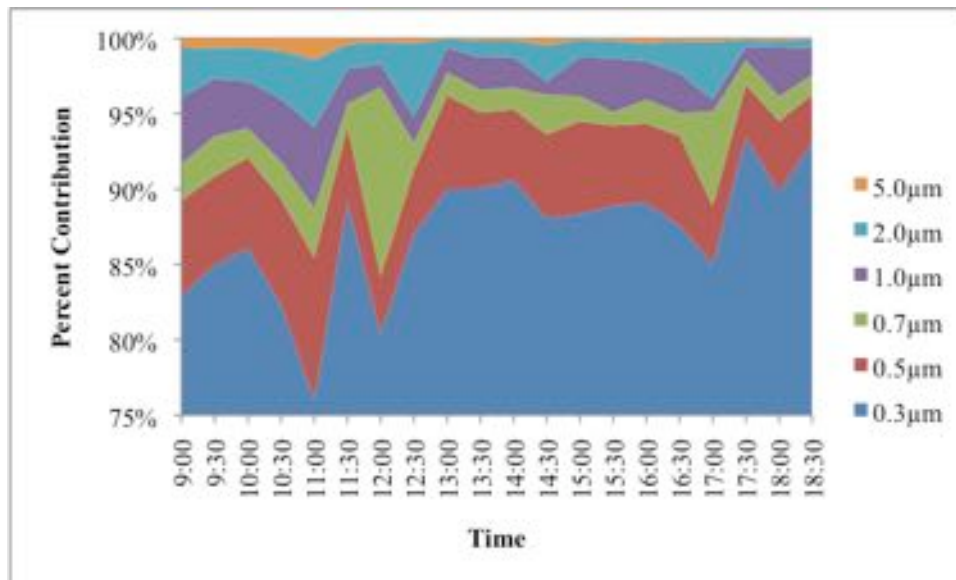
**Figure 4.14 – Average Percent Contributions for Particles sized 0.3-5.0 μm at the Monivong Boulevard Comfort Star Location on June 22, 2008**

Shown in Figure 4.15 is the average percentage that each size fraction contributes to the PM<sub>0.3-5.0</sub> particle counts at the Monivong Boulevard Comfort Star Location on June 23, 2008. Particles in the 0.3 μm size group are shown to contribute 87.1% of the total particles measured. Particles sized 0.5 μm make up 6.6% of the total count, while 0.7, 1.0, and 2.0 μm contribute 2, 2.5 and 1.5% respectively. Particles 5.0 μm in size contribute only 0.2% of the total amount of counted particles.



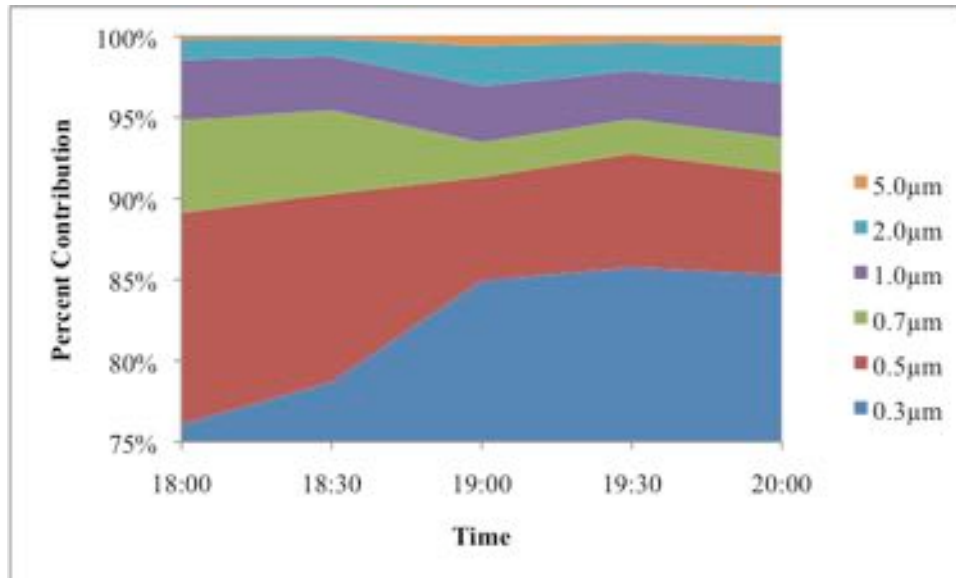
**Figure 4.15 – Average Percent Contributions for Particles sized 0.3-5.0 μm at the Monivong Boulevard Comfort Star Location on June 23, 2008**

Because temporal fluctuations also exist between each size fraction, it is necessary to understand the degree of fluctuations over the course of the day. Figure 4.16 displays the temporal variations in size fractions for particles sized 0.3-5.0 μm. Again, the 0.3 μm size fraction makes up the majority of the recorded particles. As particle size increases, the percent contribution decreases. While some large fluctuations are apparent in the percent contribution of particle sizes displayed in Figure 4.16, particles sized 0.3 μm increase by approximately 10% from 0900 hours to 1830 hours, while every other particle size fraction appears to fall to a lower concentration at the end of the sampling period in relation to the beginning.



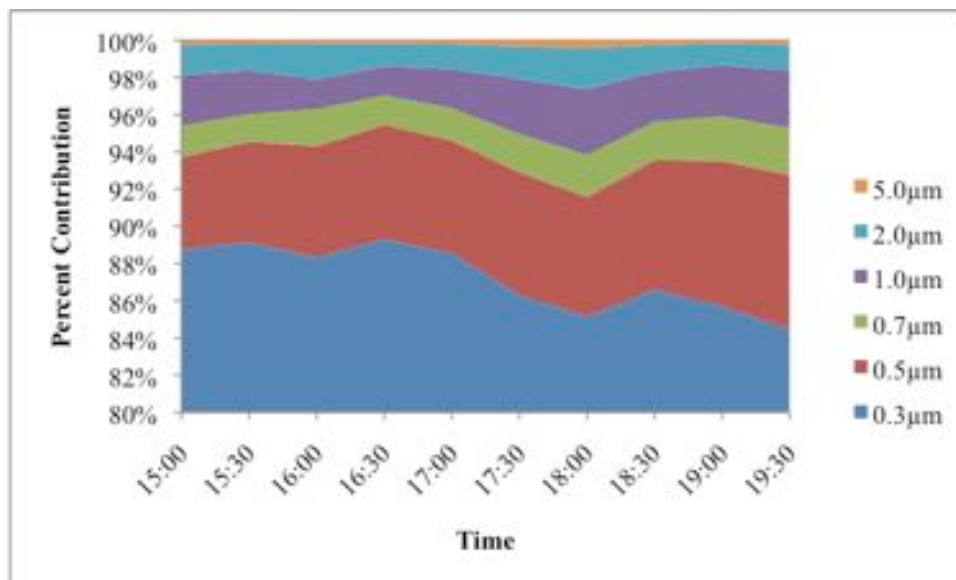
**Figure 4.16 – Average Temporal Percent Contributions for Particles sized 0.3-5.0  $\mu\text{m}$  at the Olympic Stadium location on June 22, 2008**

Figure 4.17 shows the temporal fluctuations for each size fraction throughout the entire sampling period for particles sized 0.3-5.0  $\mu\text{m}$ . The 0.3  $\mu\text{m}$  size fraction makes up the majority of the recorded particles and again, as particle size increases, the percent contribution decreases. An interesting observation is that the percent contribution of the particles sized 0.3  $\mu\text{m}$  increases from 1800 to 1900 hours while particles size 0.5 and 0.7  $\mu\text{m}$  noticeably decrease. Particles 1.0  $\mu\text{m}$  in size appear to remain around the same concentrations, while particles 2.0 and 5.0  $\mu\text{m}$  in size also appear to have a higher percent contribution at the end of the sampling time than in the beginning. The reason for this result may be that increased traffic at this location near the outer edges of Phnom Penh at night provide higher levels of fine particles, and in turn, more re-entrainment of dust by vehicles.



**Figure 4.17 – Average Temporal Percent Contributions for Particles sized 0.3-5.0  $\mu\text{m}$  at the Monivong Boulevard Comfort Star Location on June 22, 2008**

Figure 4.18 displays the temporal percentage contribution for each size fraction in the six-channel particle counter's measurements. It is shown that as the day progresses, particles 0.5  $\mu\text{m}$  in size make up an increasing percentage of the total, although particles 0.3  $\mu\text{m}$  in size are obviously the dominant size fraction, and as seen previously in Figures 4.16 and 4.17, the smaller the particle, the higher it's total contribution to the total amount of particles counted.



**Figure 4.18 – Average Temporal Percent Contributions for Particles sized 0.3-5.0  $\mu\text{m}$  at the Monivong Boulevard Comfort Star Location on June 23, 2008**

Table 4.2 aggregates the percent contribution of each particle size bin as measured with the six-channel particle counter. While the six-channel particle counter was used only three times at two unique sample sites, it is important to note that the percent contribution of each size fraction is fairly consistent. The smallest particles (0.3  $\mu\text{m}$ ) make up the majority of particle measured (81-87%) and the largest particles (5.0  $\mu\text{m}$ ) contribute the least to the overall concentration (0.2-0.4%). The smaller the particle size, the less significant the contribution of the particle size to the overall concentration. The only exception for this rule occurs at the Monivong Boulevard location on June 23 when particle 1.0  $\mu\text{m}$  in size are shown to have a higher concentration (2.5%) than those 0.7  $\mu\text{m}$  in size (2.0%).

**Table 4.2 - Percent Contribution of Particle Size Fractions**

	<i>Monivong Blvd. June 23</i>	<i>Olympic Stadium June 22</i>	<i>Monivong Blvd. June 22</i>
0.3 $\mu\text{m}$	87.1	87.4	80.9
0.5 $\mu\text{m}$	6.6	5.3	9.8
0.7 $\mu\text{m}$	2.0	2.6	4.0
1.0 $\mu\text{m}$	2.5	2.5	3.4
2.0 $\mu\text{m}$	1.5	1.9	1.6
5.0 $\mu\text{m}$	0.2	0.4	0.3

### 4.3 Temporal Particle Count Profiles

The longest roadside temporal [profile](#) was on [monitored on](#) June 15, 2008 at Monivong Boulevard, located at the Comfort Star Hotel (see Figure 3.5). The mean particle count for this sample site was  $8.48 \times 10^8$  particles/m<sup>3</sup> with a median count of  $8.28 \times 10^8$  particles/m<sup>3</sup> and a standard deviation of  $8.28 \times 10^8$  particles/m<sup>3</sup>. Particles were counted in half-hour increments from 0500 to 1900 hours, incorporating morning, afternoon and evening traffic flow. As shown by the solid line in Figure 4.19, PM<sub>10</sub> levels rose above a base count of  $6.95 \times 10^8$  particles/m<sup>3</sup> through the morning, reaching a peak at  $1.21 \times 10^9$  particles/m<sup>3</sup> at 1000 hours (an increase in particles of 73% over a 3.5-hour period). With some fluctuation the counts level out for a few hours.

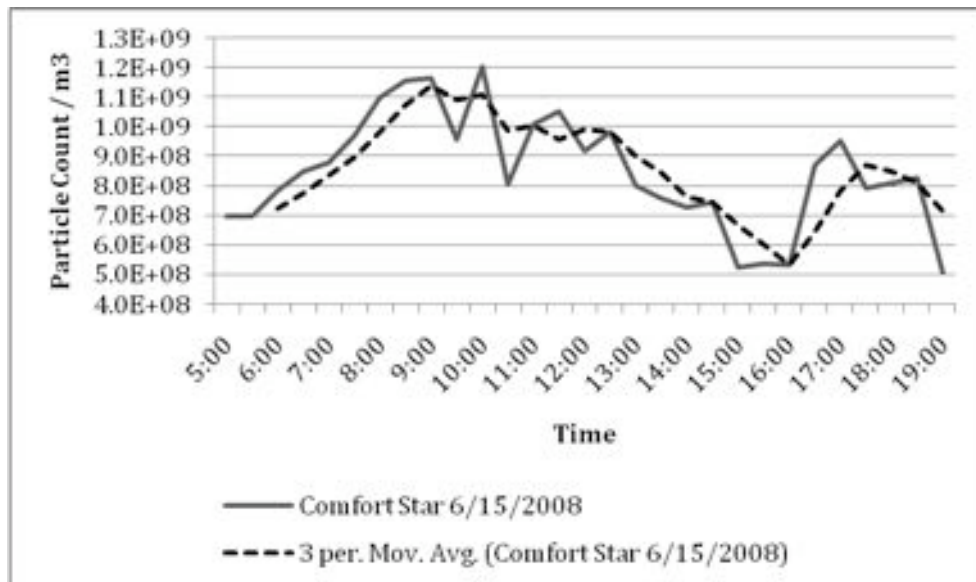


**Figure 4.19 – Temporal Particle Counts for Monivong Boulevard Comfort Star Location on June 15, 2008**

The particle counts trend downward through the day, hitting a low count of just  $5.24 \times 10^8$  particles/m<sup>3</sup>. A late afternoon increase in particle counts is observed at 1700 hours, peaking at  $9.52 \times 10^8$  particles/m<sup>3</sup>, and lasting only a few hours before returning to a base level of  $5.05 \times 10^8$  particles/m<sup>3</sup>.

A three period moving average was used to smooth out the rapid fluctuations of particle counts shown previously in Figure 4.19, and display a more appropriate representation of the average ambient concentrations. The trend line is superimposed on top of the raw data points in Figure 4.19 and is represented as a dotted line. The moving average trend displays a pronounced particle count peak lasting ten hours as well as another smaller peak in the afternoon/early evening.

Using the moving average trend line to examine particle count concentrations shows that this location represents a commuter pattern. Vehicles entering the city in

the morning (0500 hours) cause particle counts to rise until a peak is reached (0900 hours). This pattern showcases the morning rush hour pattern experienced by this major road. The evening rush hour traffic at this location is seen when particle count levels again rise from 1600 hours to 1730 hours. This location's proximity to the city's southern border and Monivong Boulevard's status as a major road linking the countryside to the urban center reinforces the interpretation of the particle count trends shown in Figure 4.19.

A second example of the late afternoon/early evening drop in particle count levels is seen in Figure 4.20, taken at the same location on June 20, 2008. The mean particle count for this sample site was  $9.47 \times 10^8$  particles/m<sup>3</sup> with a median count of  $9.87 \times 10^8$  particles/m<sup>3</sup> and a standard deviation of  $2.41 \times 10^8$  particles/m<sup>3</sup>.

The particle count levels beginning at 1700 hours rise slightly, before dropping on subsequent samples. This trend mirrors the trend displayed by particle samples taken on June 15, 2008, five days earlier, although the trend is seen on June 15 a half hour earlier than it does on June 20.

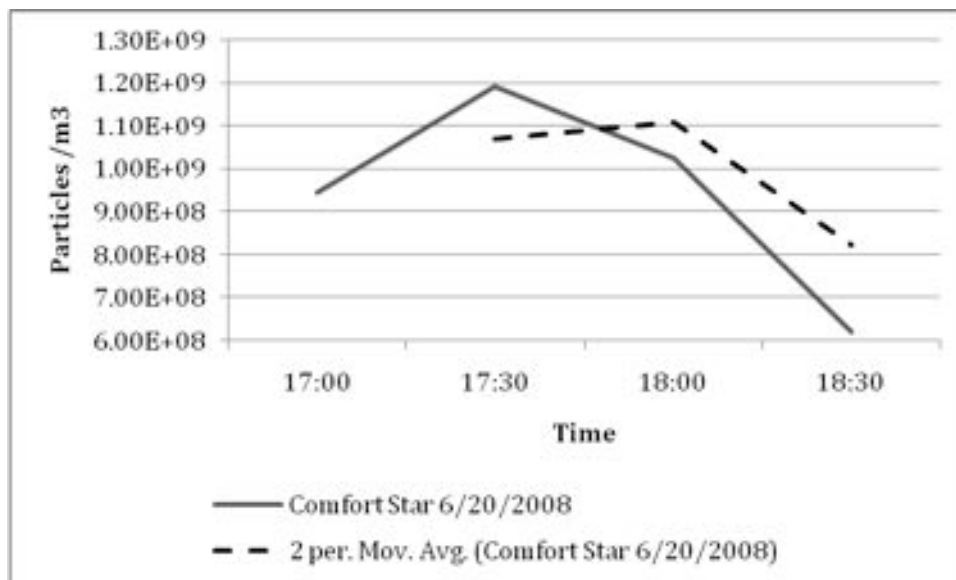


**Figure 4.20 – Temporal Particle Counts for Monivong Boulevard Comfort Star Location on June 20, 2008**

Particle counts recorded on June 17, 2008 Russian Boulevard ([see](#) Figure 3.5) have a mean particle count of  $5.67 \times 10^8$  particles/m<sup>3</sup>, a median count of  $5.83 \times 10^8$  particles/m<sup>3</sup> and a standard deviation of  $7.79 \times 10^8$  particles/m<sup>3</sup>.

The particle counts display a trend in particle counts that is very similar to the counts taken previously on Monivong Boulevard (see Figure 4.19). As shown in Figure 4.21, the 0900 hour counts are the among the highest of the day ( $6.72 \times 10^8$  particles/m<sup>3</sup>), with an exception occurring at 1400 hours ( $7.14 \times 10^8$  particles/m<sup>3</sup>), followed by a decrease of 69% in particle counts until 1600 hours when levels reach  $4.62 \times 10^8$  particles/m<sup>3</sup>.

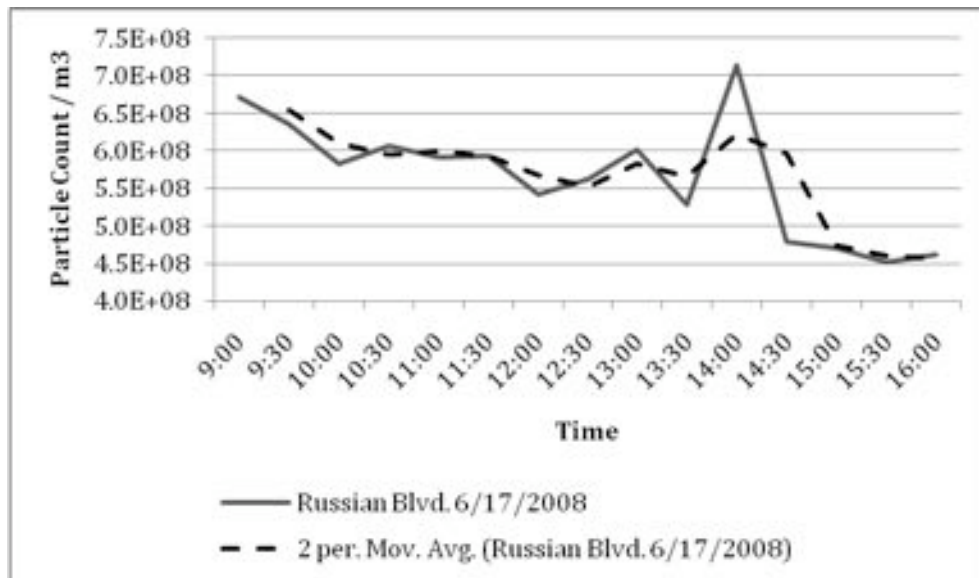


**Figure 4.21 – Temporal Particle Counts for Russian Boulevard Location on June 17, 2008**

The rationale for this steady decline is apparent when compared to the Monivong Boulevard counts opposite the Comfort Star Hotel (Figure 4.19): the counts at 0900 hours represent the penultimate apex in the morning rush hour counts, while 1600 hours represents the lowest count as a result of decreased business and commuting traffic in the late afternoon/early evening. In other words, the early counts on Russian Boulevard show the back-end of the morning commute traffic while the spike at 1330 hours and subsequent drop in particle counts represent an increase in traffic earlier in the day than those seen previously in Figure 4.19. The spike shown at 1330 hours appears to be short-lived and may be indicative only of a localized disturbance, as the overall trend continues downward after the spike is seen.

Adding a 2-period moving average trend line to Figure 4.21 smoothes over the aggressive spikes in particle counts, and helps to visualize the two distinct groupings of particle counts. The moving average trend line in Figure 4.21 shows a smoother transition from falling particle counts after 900 hours to the elevated counts in the afternoon, to their eventual drop off into the evening hours.

Particle counts were taken at the intersections of Monivong and Sihanouk Boulevard ([see](#) Figure 3.5). The mean particle count for this sample site was  $6.69 \times 10^8$  particles/m<sup>3</sup> with a median count of  $5.83 \times 10^8$  particles/m<sup>3</sup> and a standard deviation of  $2.83 \times 10^8$  particles/m<sup>3</sup>.

Temporal particle counts are shown in Figure 4.22. The 0900 hour count ( $6.72 \times 10^8$  particles/m<sup>3</sup>) may represent a decrease from possibly higher rush-hour counts and the particle counts appear stabilize at an average of  $5.77 \times 10^8$  particles/m<sup>3</sup> throughout the morning from 1000 hours to 1330 hours. Through the afternoon there appears to be a greater fluctuation in counts, including a particle count spike of 74% from 1330 to 1400 ( $5.30 \times 10^8$  to  $7.14 \times 10^8$  particles/m<sup>3</sup>) hours followed by a general decrease in concentrations which may signify the early afternoon commute traffic.

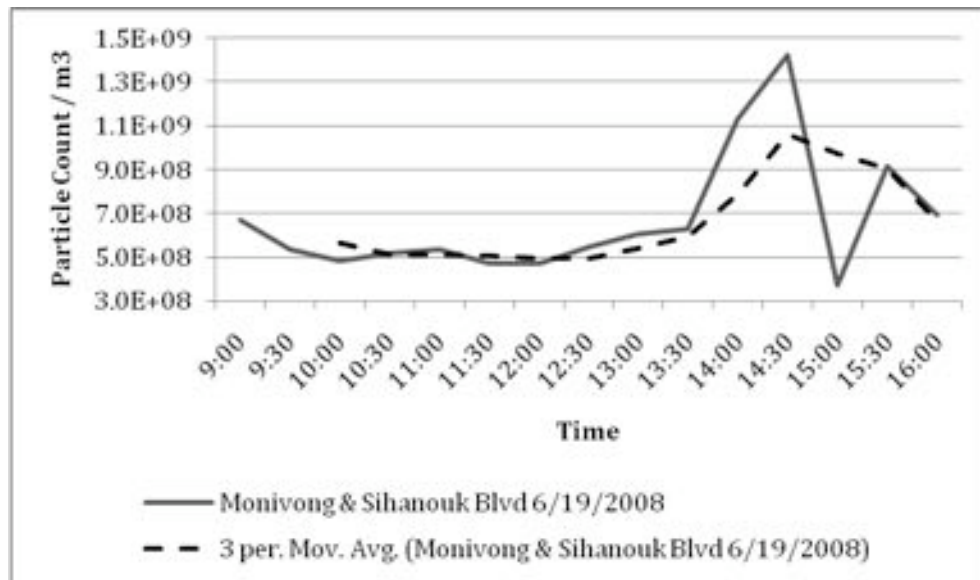


**Figure 4.22 – Temporal Particle Counts for Intersection of Monivong and Sihanouk Boulevards  
Location on June 17, 2008**

When the counts are graphed using a 3-period moving average it is immediately apparent that after staying within a similar range, the particles begin to rise at 1330 hours, reach a peak of  $5.30 \cdot 10^8$  particles/m<sup>3</sup> at 1430 hours, then begin to decline until sampling is completed at 1600 hours with a particle concentration of  $4.62 \cdot 10^8$  particles/m<sup>3</sup>.

Temporal profiles at the central market and waterfront in Phnom Penh (see Figure 3.5) were taken on June 20, 2008 at one-hour intervals. Because the two locations are within walking distance of each other, and they represent very different urban scenarios, the decision was made to sample both locations on the same day at alternating hour intervals rather than half-hour intervals as conducted with the other profiles. The central market location was sampled on the full-hour intervals from

0900 to 1600 hours, while the waterfront location was sampled on the half-hour intervals from 0930 to 1530 hours. The two locations provided very different particle count trends as per their different environments.

The central market had a mean particle count of  $8.64 \times 10^8$  particles/m<sup>3</sup>, a median count of  $8.24 \times 10^8$  particles/m<sup>3</sup> and a standard deviation of  $2.49 \times 10^8$  particles/m<sup>3</sup>.

Temporal particle counts for the central market sampling site can be seen in Figure 4.23. The central market is a very busy area in the center of Phnom Penh and had high particulate levels in the morning that rapidly dropped from  $1.03 \times 10^9$  to  $7.24 \times 10^8$  particles/m<sup>3</sup> (900 to 1000 hours), before climbing at midday from  $7.37 \times 10^8$  to  $9.95 \times 10^8$  particles/m<sup>3</sup> (1100 to 1200 hours), and then dropping again into the afternoon from  $1.00 \times 10^9$  to  $7.77 \times 10^8$  particles/m<sup>3</sup> (1300 to 1500 hours). The pattern shown in Figure 4.23 differs from those shown at previous locations in that a mid-day peak is obvious. This peak may represent inner-city traffic based upon a busy shopping and business district that experiences large volumes of traffic in at mid-day rather than commuter traffic in either the morning or the evening.

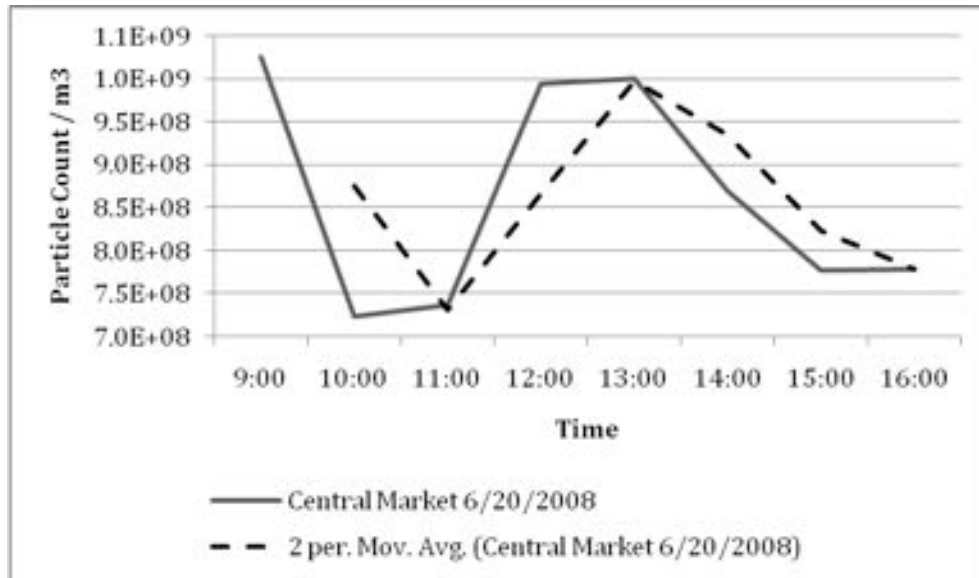


**Figure 4.23 – Temporal Particle Counts for Central Market Location on June 20, 2008**

Adding a 2-period moving average trend line does little to smooth the aggressive changes in observed particle counts, however, the trend line does help to distinguish two behaviors of particle counts throughout the day. Like the Monivong Boulevard Comfort Star Hotel location (Figure 4.19) and the Russian Boulevard (Figure 4.22) decrease in particle counts in the morning (after 0900 hours) may be attributed to the end of the morning rush hour traffic, while the rise and subsequent fall of particle counts later in the day may denote the beginning and end of the afternoon rush hour.

The waterfront located on the banks of the Tonle Sap River, is a less busy location than the heavily trafficked central market. The mean particle count for this sample site was  $5.50 \times 10^8$  particles/m<sup>3</sup> with a median count of  $6.11 \times 10^8$  particles/m<sup>3</sup> and a standard deviation of  $2.49 \times 10^8$  particles/m<sup>3</sup>.

Temporal particle counts recorded at the waterfront (Figure 4.24) showed a general decline in particulate levels all day until 1430 hours from  $7.79 \times 10^8$  to  $4.29 \times 10^8$  particle/m<sup>3</sup> (a decrease of 55%) when levels began to rise, likely with the evening commute traffic. Air quality issues may less impact the waterfront than other inner-city locations, as a constant breeze off of the rivers may keep pollution originating from city sources from reaching the waterfront. While not deserted by any means, the waterfront experiences less vehicle traffic travelling at slower speeds than many others sampled locations, which may also lead to the downward-sloping particle trend shown. Superimposing a two-period moving average trend line onto the particle counts graphed previously in Figure 4.24, it can be seen that particle counts at the waterfront exhibit a trend of decreasing counts from the morning high values. This decline in particle counts may be a function of wind speed, as wind speeds tend to increase throughout the day.

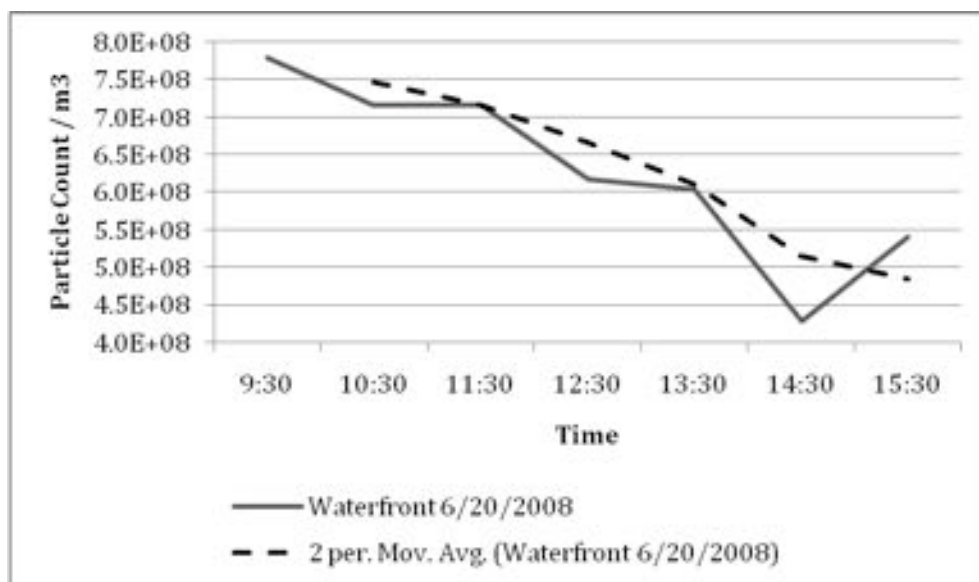
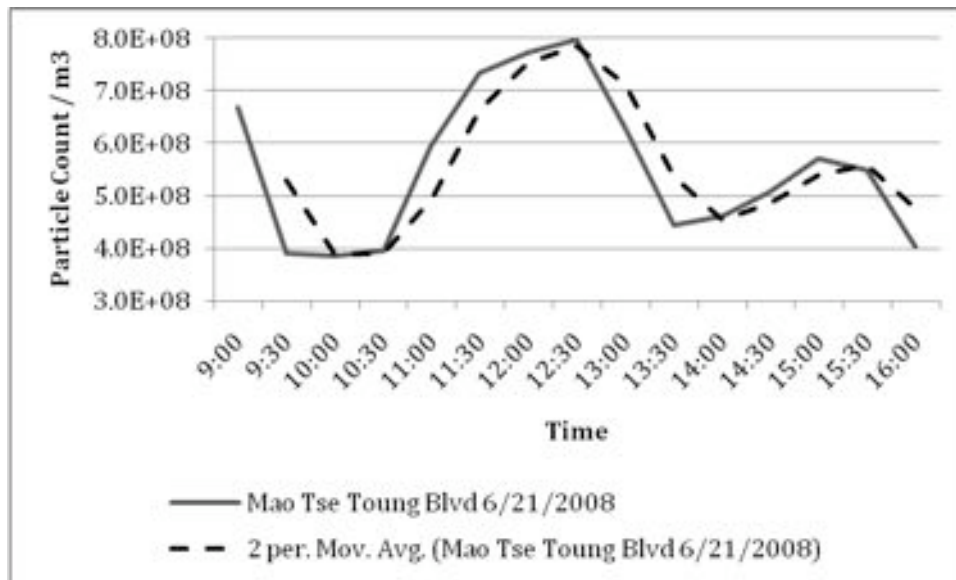


Figure 4.24 – Temporal Particle Counts for Waterfront Location on June 20, 2008

An area in East Phnom Penh on Mao Tse Toung Boulevard ([see](#) Figure 3.5) was profiled on June 21, 2008, from 0900 to 1600 hours. The mean particle count for this sample site was  $5.54 \times 10^8$  particles/m<sup>3</sup> with a median count of  $5.50 \times 10^8$  particles/m<sup>3</sup> and a standard deviation of  $1.43 \times 10^8$  particles/m<sup>3</sup>.

The temporal particle count profile is shown in Figure 4.25 shows particle count trends that combine those features found in Figures 4.19 and 4.21 - distinctive morning and evening rush hours, as well as high mid-day traffic counts.

Figure 4.25 shows a 58% decrease in particle counts from approximately  $6.69 \times 10^8$  to  $3.90 \times 10^8$  particles/m<sup>3</sup> from 0900 to 0930 hours before they level off for an hour (likely the tail end of the morning rush hour). Particle counts rise 50% from 1030 to 1230 hours (from  $3.96 \times 10^8$  to  $7.89 \times 10^8$  particles/m<sup>3</sup>). Particle counts fall again from 1230 to 1330 hours to  $4.44 \times 10^8$  before rising until another peak is reached at 1500 hours ( $5.70 \times 10^8$ ). After superimposing a 2-period moving average trend line onto Figure 4.25, it is apparent that a similar pattern can be extracted from Figure 4.19, although the particulate levels at that location are seen to fluctuate more than the levels in Figure 4.25. This location also shows a less pronounced (and earlier) evening rush hour rise in particle levels than Figure 4.19.



**Figure 4.25 – Temporal Particle Counts for Mao Tse Toung Location on June 21, 2008**

Particle Counts taken at the Olympic Stadium sample site (see Figure 3.5) are shown in Figure 4.26. This location, a deep inner-city business area, is heavily trafficked with business traffic (store, shop and restaurant traffic), as well as through-traffic (commuters). The mean particle count for this sample site was  $4.30 \times 10^8$  particles/m<sup>3</sup> with a median count of  $3.66 \times 10^8$  particles/m<sup>3</sup> and a standard deviation of  $2.10 \times 10^8$  particles/m<sup>3</sup>.

Particulate levels from 0900 hours to 1700 hours fluctuate between around  $3.0 \times 10^8$  and  $5.5 \times 10^8$  particles/m<sup>3</sup>. Particle concentrations at the end of the sampling period (1830 hours) are 37% higher than those seen at the start of sampling (0900 hours). The fluctuations in particle counts show that an evening rush hour is apparent, while the low, stagnant particle counts in the morning may have missed the morning commuter traffic prior to 0900 hours.

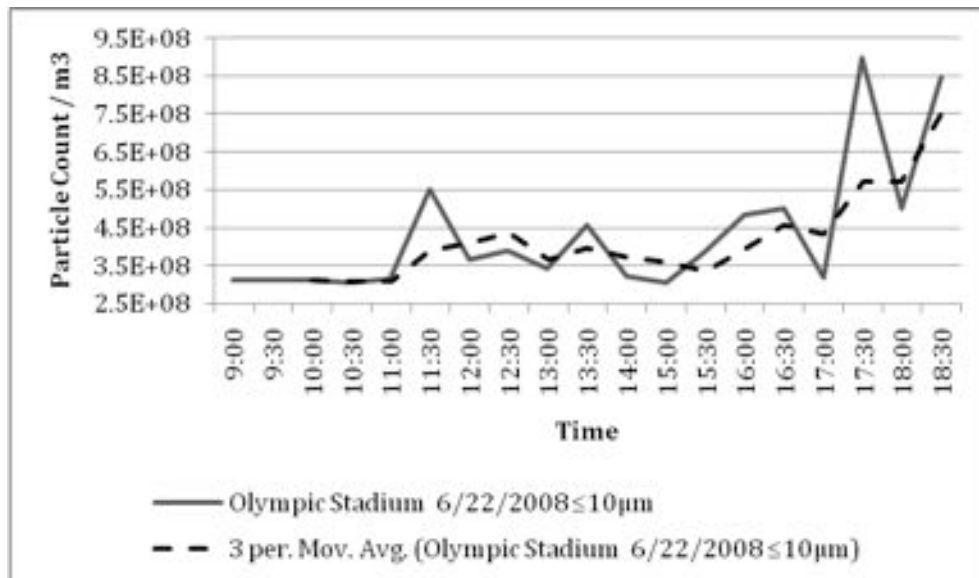


Figure 4.26 – Temporal Particle Counts for Olympic Stadium Location on June 21, 2008

When the fluctuations of the particle counts are smoothed over using a three-period moving average trend line superimposed on the data in Figure 4.26, it is seen that particle count levels experience a small rise in the afternoon perhaps due to regular inner-city traffic patterns. Particle count levels increase from 1500 hours onward at this location showing the evening rush hour traffic. The particle counts recorded at this location may be a weaker (i.e. less exaggerated) example of the profile presented for the intersection of Monivong and Sihanouk Boulevards in Figure 4.22.

Particle counts were taken at the intersection of Russian Boulevard and Street 315 near the Royal University of Phnom Penh, in the Northwest corner of the city (see Figure 3.5). The mean particle count for this sample site was  $5.50 \times 10^8$  particles/m<sup>3</sup> with a median count of  $5.21 \times 10^8$  particles/m<sup>3</sup> and a standard deviation of

$1.35 \times 10^8$  particles/m<sup>3</sup>.

The temporal particle count trend is shown in Figure 4.27. Recorded from 0900 to 1530 hours, the profile shows a similar pattern to Figures 4.19, 4.21, 4.22, and 4.23, with 0900 hours representing the tail end of the morning commute traffic ( $8.87 \times 10^8$  particles/m<sup>3</sup>) and falling until 1230 hours ( $4.29 \times 10^8$  particles/m<sup>3</sup>), and afternoon commute traffic clearly defined as an increase (1200 hours to 1430 hours) followed by a decrease in particulate counts (1430 hours to 1530 hours). This location clearly shows an early afternoon rush hour. The rise in particle counts from 1230 to 1430 hours may signify an earlier version of the evening rush hour shown in Figure 4.19. This location displays a trend much like the trend shown previously at the Russian Boulevard sample site shown in Figure 4.21.

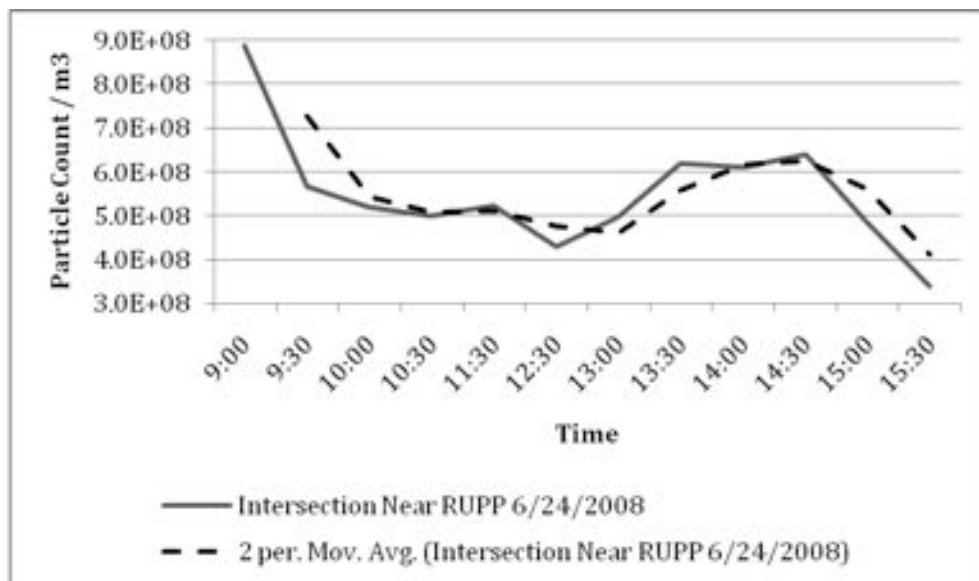


**Figure 4.27 – Temporal Particle Counts for Intersection of Russian Boulevard and Street 315 on June 21, 2008**

Table 4.3 displays the mean, median and standard deviation of PM<sub>10</sub> particle

counts for each location sampled in the 2008 wet season. Mean particle counts ranged from  $4.30 \times 10^8$  particles/m<sup>3</sup> at the Olympic Stadium location on June 22, 2008 (shown in Table 4.3 in dark gray) to  $1.02 \times 10^9$  particles/m<sup>3</sup> at the Monivong Boulevard Comfort Star Hotel location on June 22, 2008 (shown in Table 4.3 in light gray), a difference of 60% at between two locations measured on the same day separated by only approximately 2.85 kilometers. The large difference in particle counts is due to the fact that the locations were sampled at different times of day, 0900 to 1400 hours for the Olympic Stadium and 1800 to 2000 hours for the Monivong Boulevard Comfort Star Hotel location.

**Table 4.3 – Mean, median and standard deviation of PM<sub>10</sub> particle counts**

<i>Site</i>	<i>Mean</i>	<i>Median</i>	<i>Standard Deviation</i>
Comfort Star 6/15/2008	8.48E+08	8.28E+08	1.92E+08
Russian Blvd. 6/17/2008	5.67E+08	5.83E+08	7.79E+07
Monivong & Sihanouk Blvd 6/19/2008	6.69E+08	5.47E+08	2.83E+08
Central Market 6/20/2008	8.64E+08	8.24E+08	1.27E+08
Waterfront 6/20/2008	5.50E+08	6.11E+08	2.49E+08
Comfort Star 6/20/2008	9.47E+08	9.87E+08	2.41E+08
Mao Tse Toung Blvd 6/21/2008	5.54E+08	5.50E+08	1.43E+08
Olympic Stadium 6/22/2008	4.30E+08	3.66E+08	2.10E+08
Comfort Star 6/22/2008	1.02E+09	1.13E+09	3.61E+08
Comfort Star 6/23/2008	8.55E+08	8.66E+08	1.19E+08
Russian Blvd. & Street 315 6/24/2008	5.50E+08	5.21E+08	1.35E+08

Different traffic patterns exist at different times of the day, and are encompassed in three groups. The first is a typical commuting pattern with high

particle count values in the morning and late afternoon, as seen in Figures 4.19, 4.23, 4.25 and 4.27. These locations are all situated near the edge of the city, and serve as commuting roads bringing vehicles in and out of the city center. A second traffic pattern seen is defined as city-traffic that shows high values near the middle of the day when the majority of business is conducted in the business centers. This pattern is seen in Figures 4.22, and 4.26, locations within the inner parts of the city. The third distinguishable traffic pattern is described as a pattern that has a steady decline of particle count levels from the morning rush-hour levels. This pattern can be seen in Figures 4.21 and 4.24. While the decrease in particle counts at the Russian Boulevard location (Figure 4.21) is attributed to a lower amount of vehicles throughout the day coupled with a lower afternoon rush hour than other sites, the waterfront location's (Figure 4.24) decreasing trend of particle counts is attributed to wind coming off the river.

#### **4.4 Particle Mass and Particle Count Correlation**

The high-volume sampler was run concurrent with a particle counter at the RUPP site to determine if a relationship between particle counts and mass loadings can be obtained. Particle counts were taken at the beginning and end of each high-volume sampling period, and averaged. Six comparative data sets were obtained, and are shown in Table 4.4. For quality control assurance purposes, some particle counts were subsequently replicated after the first particle count was taken. Multiple particle counts were averaged, before a total average for that day was made.

**Table 4.4 – Start, End and Total Mean Particle Counts for High-Volume Sampler Runs**

<i>Date</i>	<i>Mean Start Count</i>	<i>Mean End Count</i>	<i>Total Mean Count</i>
6/17/08	$6.20 \times 10^8$	$6.83 \times 10^8$	$6.51 \times 10^8$
6/19/08	$5.06 \times 10^8$	$2.95 \times 10^8$	$4.01 \times 10^8$
6/20/08	$7.81 \times 10^8$	$5.07 \times 10^8$	$6.44 \times 10^8$
6/21/08	$4.15 \times 10^8$	$5.09 \times 10^8$	$4.62 \times 10^8$
6/22/08	$3.24 \times 10^8$	$3.52 \times 10^8$	$2.94 \times 10^8$
6/23/08	$3.26 \times 10^8$	$2.83 \times 10^8$	$3.01 \times 10^8$

Values recorded using the laser particle sampler were generally in the expected range, with the exception of a particle sample taken at the end of the first sampling period. This measurement appears to be anomalous as its count exceeded the morning count and is 57% greater than the average end reading for every other sampled day. Because the recorded particle count of 241,321 particles ( $6.83 \times 10^8$  particles/m<sup>3</sup>) is likely artificially elevated, and is 57% greater than the average end count for all other days, the particle count in question was not included in the proceeding calculations. As each sample recorded with the laser particle counter represents only a minute in time, it is possible that the one-minute sample taken does not represent the overall air quality at the site, which can be artificially raised by the passing of a single vehicle. Although a count with a value of 276,027 ( $7.81 \times 10^8$  particles/m<sup>3</sup>) was recorded at the start of sampling on June 20, 2008, the end of sampling particle count shows a downward trend in particle counts as expected, and was not deemed an outlier.

Particle mass loadings, derived from the analysis of the high-volume air sampler filters, along with the averaged particle counts, derived from the particle counter, were graphed on a scatter plot (Figure 4.28). A linear regression trend superimposed on the scatter plot displays an  $R^2$  value of 0.61551. Using the trend line's formula of  $y = 4^{-8}(x) + 19.022$  it is possible to predict the mass represented by a specific particle count to a certainty of 62%. In other words, the regression line accounts for 62% of the value of particle mass as caused by particle count values.

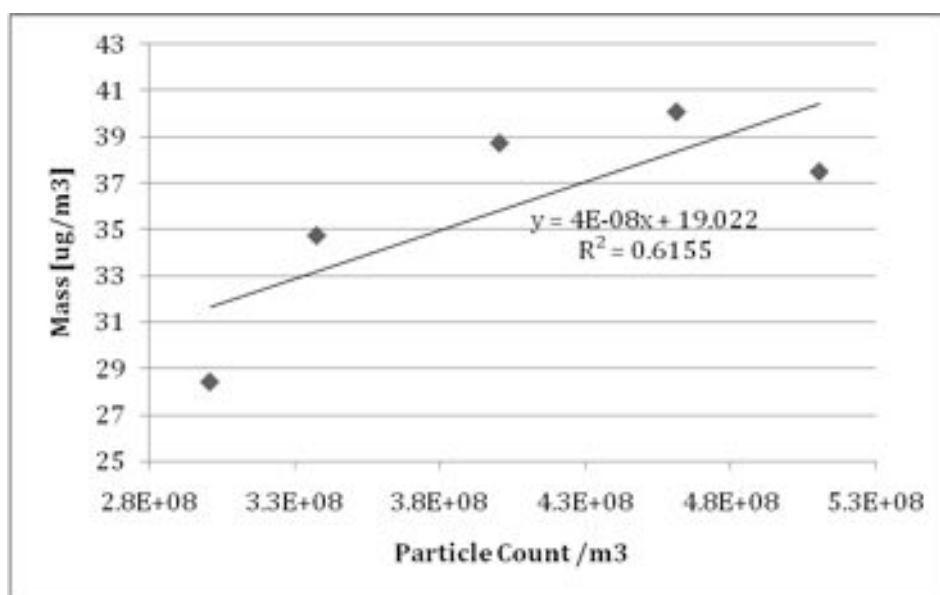


**Figure 4.28 – Particle Mass and Number Count Correlation**

Using the information presented above and in Figure 4.28, it is possible to convert temporal particle count profiles to temporal profiles displaying particle mass, the preferred measurement unit of airborne particles in EPA and WHO standards as displayed in Figure 2.1. Figure 4.29 displays the same temporal profile shown previously in Figure 4.19, but using the above formula transposes the y-axis units from volume (particles/m<sup>3</sup>) to mass (μg/m<sup>3</sup>). The WHO 24-hour PM<sub>10</sub> mean guideline of 50 μg/m<sup>3</sup> is shown in Figure 4.29 as a red line, intended to show how the hourly

mass calculation compares with the guideline. While the measurements were not taken for a full 24-hour period, comparing the WHO guideline to the measured mass can help to distinguish any inordinately high mass concentrations. The mean concentration for the 14-hour sampling shown in Figure 4.29 is  $53 \mu\text{g}/\text{m}^3$ ,  $3 \mu\text{g}/\text{m}^3$  above the WHO 24-hour  $\text{PM}_{10}$  mean and much lower than the EPA 24-hour  $\text{PM}_{10}$  mean of  $150 \mu\text{g}/\text{m}^3$ .

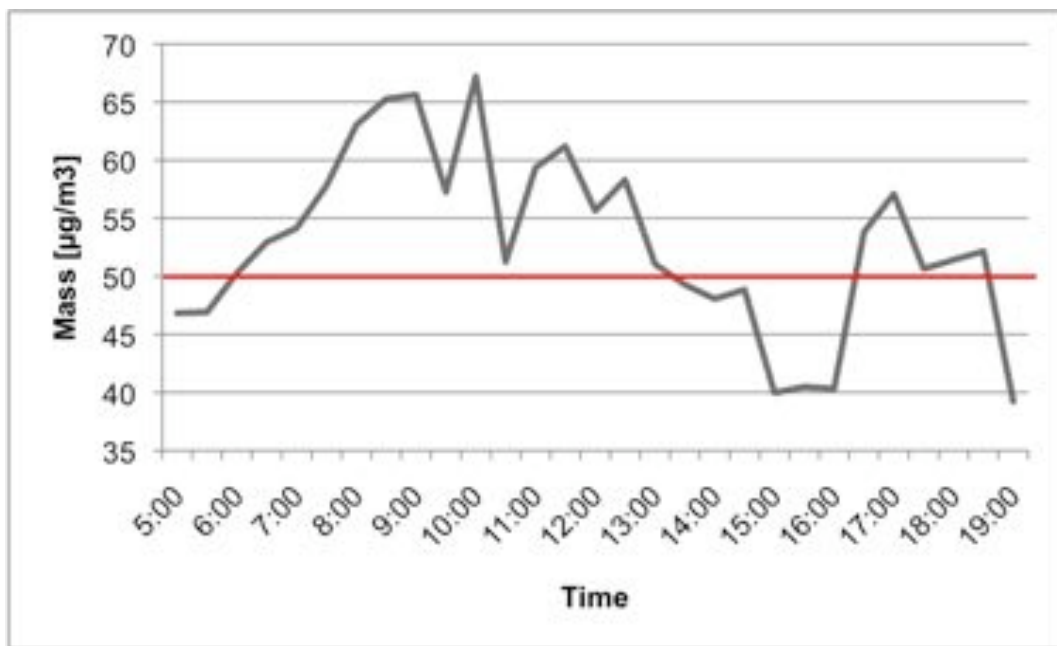


**Figure 4.29 – Temporal Particle Mass Measurements for Monivong Boulevard Comfort Star Location on June 15, 2008**

Dasgupta, et al., (2005) estimates average citywide  $\text{PM}_{10}$  levels in Phnom Penh as  $64\text{--}71 \mu\text{g}/\text{m}^3$ . The measured and predicted counts shown at each location appear to be in line with expected mass values as reported in the literature and reviewed in Chapter 2 of this paper (Monkkonen et al., 2004; Dasgupta, et al., 2005).

#### 4.5 Road Dust Elemental Composition

Road dust was collected from seven sites in Phnom Penh and three sites in a nearby rural province. All samples were analyzed with an FPXRF unit. Shown in Figure 4.30 is the total mean concentration of all analyzed road dust samples for urban and rural Phnom Penh on a logarithmic scale.

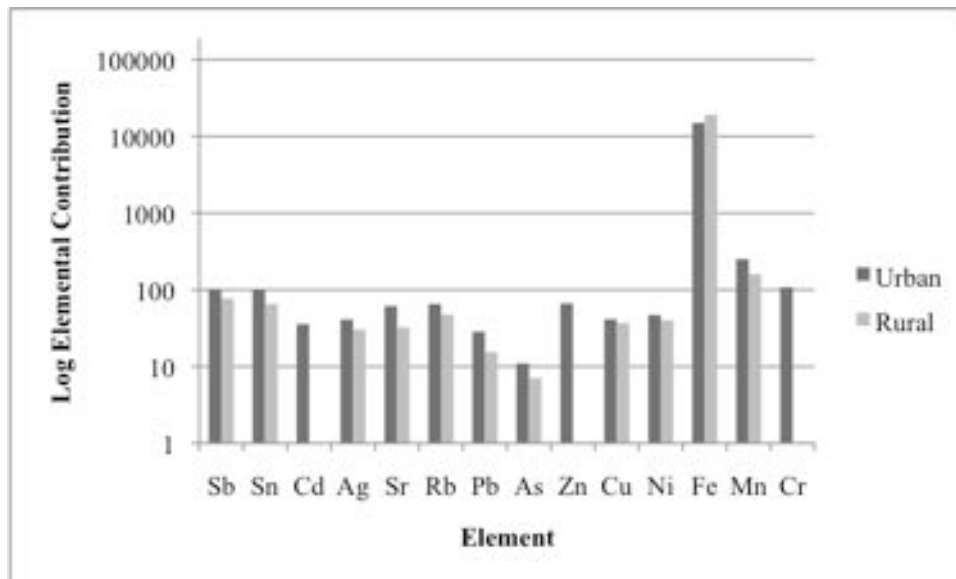


Figure 4.30 - Elemental Composition of Urban and Rural Road Dust Samples

The concentrations are in general agreement, with the exception of one rural sample site (RDI). This site exhibited elevated concentrations of Fe, Mn and Cr.) A brick factory is located in proximity to the sample site and a subsequent inspection has shown that broken brick pieces are used as fill. This sample site was excluded from the all calculations.

Most elements recorded are in concentrations less than 100 or 50 ppm, and do not make up a significant portion of the sample individually. Iron (Fe) and Manganese (Mn) are the dominant elements in both sets of road dust samples. Table 4.5 shows the concentration of elements in both urban and rural road dust in ppm. It

can be seen that Fe and Mn clearly dominate the concentration. It should also be noted that in no instance does an element appear in greater concentrations in the rural samples than the urban samples, suggesting that the rural material may be transported into the city and deposited, or in other words that the rural sediment is the source of the urban sediment.

**Table 4.5 – Mean Urban, Rural and Global Crustal Abundance of Measured Elements in ppm**

<i>Element</i>	<i>Mean urban concentration</i>	<i>Mean rural concentration</i>
Sb	102.1	77.2
Sn	99.9	65.6
Cd	35.7	N/A
Ag	41.1	30.5
Sr	61.4	32.3
Rb	65.4	47.3
Pb	28.5	15.4
As	11.0	7.1
Zn	66.4	N/A
Cu	41.4	36.9
Ni	46.9	40.2
Fe	147,974.4	19,103.6
Mn	251.7	159.9
Cr	107.9	N/A

#### **4.5.1 Enrichment Factors**

Enrichment factors were calculated using mean urban, rural and bulk deposition material concentrations. Table 4.6 contains the urban, rural and bulk deposition concentrations in parts per million (ppm) of elements measured with the FPXRF unit.

**Table 4.6 – Mean concentration in ppm of Urban, Rural and Bulk Deposition Material**

<i>Element</i>	<i>Mean Urban Concentration</i>	<i>Mean Rural Concentration</i>	<i>Mean Bulk Deposition Material Concentration</i>
Sb	102.1	77.2	353.1
Sn	99.9	65.6	311.4
Cd	35.7	N/A	114.6
Ag	41.1	30.5	159.1
Sr	61.4	32.3	17.7
Rb	65.4	47.3	11.2
Pb	28.5	15.4	21.6
As	11.0	7.1	5.3
Zn	66.4	N/A	414.9
Cu	41.4	36.9	53.2
Ni	46.9	40.2	63.6
Fe	147,974.4	19,103.6	7500.0
Mn	251.7	159.9	115.7
Cr	107.9	N/A	N/A

Arsenic (As) was used as the reference element for the enrichment factor calculation because of its low but prevalent abundance in both urban and rural areas. Because Cambodia contains natural trace amounts of Arsenic, anthropogenic As enrichment is unlikely. Enrichment factors calculated for the urban road dust using the road dust collected from the rural samples as the reference material are shown in Table 4.7. As can be seen in Figure 4.7, enrichment factors much lower than 10 suggest that the urban road dust is not heavily enriched by anthropogenic means, and suggests that the rural sediment is a major source of the dust found within the city.

**Table 4.7 – Enrichment Factors for Urban Road Dust Using Rural Road Dust as Reference Material and Arsenic as Reference Element**

Element	Sb	Sn	Cd	Ag	Sr	Rb	Pb	As	Zn	Cu	Ni	Fe	Mn	Cr
EF	0.9	1.0	n/a	1.9	1.2	0.9	1.2	1.0	n/a	0.7	0.8	5.0	1.0	n/a

Enrichment factors calculated for the bulk deposition material using the road dust collected from the urban samples as the reference material are shown in Table 4.8. As can be seen in Figure 4.8, enrichment factors much lower than 10 suggest that the urban road dust is not heavily enriched by anthropogenic means. An exception to this is seen with the enrichment factor for Zinc (Zn). An EF of 12.9 suggests that this element is slightly enriched by anthropogenic means such as alloy handling or production. The EF values presented for the other elements suggest that the urban sediment is resuspended and can be considered the source bulk deposition.

**Table 4.8 – Enrichment Factors for Bulk Deposition Material Using Urban Road Dust as Reference Material and Arsenic as Reference Element**

Element	Sb	Sn	Cd	Ag	Sr	Rb	Pb	As	Zn	Cu	Ni	Fe	Mn	Cr
EF	7.2	6.5	6.6	8.0	0.6	0.4	1.6	1.0	12.9	2.7	2.8	0.1	1.0	n/a

## Chapter 5 - Observations of Particulates in Cambodia

### 5.1 Urban Particulate Observations

The streets of Phnom Penh are the centerpiece of commerce and activity. Because most of the businesses and residences in the city are at or near street level, the sidewalks and streets tend to be crowded and busy for most of the day. Paved roads tend to collect garbage and smaller amounts of road dust than dirt roads. Walking the city streets, it is immediately apparent that Phnom Penh is a city of dusty streets. Dust can be seen everywhere from the side of the street to the facades of buildings. Walkers will also notice that the air can be difficult to breathe, especially when in the street where large numbers of vehicles are accumulated. Private power generators, and outdoor charcoal stoves and grills add to the ambient levels of particulates. Many residents wear dust masks to combat the adverse air quality. In Figure 5.1, a city employee can be seen wearing a dust mask, sweeping dirt from a thoroughfare road in the city.



**Figure 5.1 – A City Worker Sweeping Dust and Garbage Debris from a Street in Phnom Penh**  
Paved thoroughfare roads inside the city tend to experience more traffic than other types of roads in the city. Because of the high density of traffic in certain locations at certain times of the day, it is not uncommon to observe commuters, workers and other people

wearing protective surgical masks to filter the dust and exhaust for one's breathing.

Figure 5.2 shows these masks in use by a variety of different people on motorbikes.



**Figure 5.2– Commuters in Phnom Penh Wearing Masks to Protect from Particulate Inhalation**

In the outer reaches of the city near the concentric ring roads surrounding the perimeter of Phnom Penh to protect from flooding, roads can be more covered with dust than those nearer the city center, as seen in Figure 5.3. It is also worth noting that heavier inner-city traffic may cause more dust to be resuspended than less busy roads. In this figure, dust buildup is seen on the side of the road, while the center of the road remains exposed, and fairly clean when compared to the side of the road, again suggesting that high traffic throughput in the center of the road may mean that this dust has already been resuspended.



**Figure 5.3 – Dust Buildup on Two Roads in Outer-Phnom Penh**

Some side streets in Phnom Penh remain unpaved and represent an entirely different scene than main roads. Side roads have less through-traffic than most other roads and as a result have larger coarse particulate concentration on the ground, although this material may not be as readily re-suspended as coarse material on other roads due to less vehicular agitation of the particulate matter. Figure 5.4 shows a side street in Phnom Penh that remains unpaved and unkempt. It can be seen in the photograph that along with large amounts of coarse material comprising the dirt road, fine particulates are also present, as cooking and burning of wood biofuels.



**Figure 5.4 – An Unpaved Side Street in Phnom Penh**

## **5.2 Rural Particulate Observations**

Rural roads outside of Phnom Penh contain the highest percentage of dirt roads, as very few if any roads are paved in villages outside of the city. Figure 5.5 shows a dirt road in a village not far outside of Phnom Penh, while Figure 5.6 shows a dirt road in a rural village approximately one-hour southeast of Phnom Penh in Kean Svay district. In both pictures, it is immediately apparent that less traffic and other anthropogenic activities are taking place on the road. It is also apparent from the photographs that the dirt on the roads in the city is a darker brown color than the bright orange colors comprising the rural roads. This corresponds to the sandy alluvial sediment prevalent near the river banks and the smaller sized clay particles that settle out away from the riverbanks in more rural areas.



**Figure 5.5 – A Dirt Road Outside Phnom Penh**



**Figure 5.6 – A Dirt Road in a Remote Rural Village**

## Chapter 6 – Summary and Conclusion

### 6.1 Conclusion

Atmospheric Particulates are used as an indicator of air quality, and a general understanding of airborne particulates in a region is crucial to understanding many of the health problems that extend or are exacerbated by large quantities of particulate matter. Southeast Asia and Cambodia suffer from a lack of data and detailed studies concerning PM, an advantage that more developed nations enjoy. The influence of local and regional influences on airborne particulates in Phnom Penh has been conclusively established in this paper.

PM concentrations in and around Phnom Penh are dependent on a confluence of three factors: spatial location of the site, traffic volume and commuting patterns. The spatial location of a chosen site dictates how particulates are acted upon by natural forces such as wind near the waterfront or the chemical composition of the particles.

Particle concentrations tend to drop off, as one gets closer to the Phnom Penh waterfront area due to persistent winds off of the rivers. Also, particles nearer the banks of the rivers tend to contain higher concentrations of sandy alluvial sediment, while particles further away contain higher concentrations of clay material.

Traffic volume tends to be a function of spatial location – a factor established by the layout of the city. Areas with higher traffic throughput are seen in the inner city areas such as the Central Market and near the city's border on roads that direct traffic into and out of the city like the Russian and Monivong Boulevards towards the airport and rural surroundings respectively.

Commuting patterns influence particulate concentrations in inner-city locations tend to experience higher traffic volumes mid-day, while locations near major commuting roads experience elevated particulate concentrations at expected commuting times (morning and evening). Three general traffic patterns can be discerned: commuter traffic, inner city traffic and a progressive downward trend.

A commuting pattern with high particle count values in the morning and late afternoon (see Figures 4.19, 4.23, 4.25 and 4.27) is seen at locations situated near the edge of the city, and serve as commuting roads bringing vehicles in and out of the city center. A second traffic pattern is defined as city-traffic that shows high values near the middle of the day (see Figures 4.22, and 4.26) within the inner parts of the city. The third traffic pattern is described as a pattern that has a steady decline of particle count levels beginning from the morning rush-hour levels (see Figures 4.21 and 4.24). While the decrease in particle counts at the Russian Boulevard location (see Figure 4.21) is attributed to a lower amount of vehicles throughout the day coupled with a lower afternoon rush hour than other sites, the waterfront location's (see Figure 4.26) decreasing trend of particle counts is attributed to wind coming off the river.

The next step to understanding particulate concentrations is to examine the size makeup and elemental composition of the measured particulates. As particle size decreases, the higher the propensity to cause or exacerbate human harm increases. High levels of coarse particles ( $> 2.0 \mu\text{m}$ ) are less dangerous than high levels of fine particulates ( $< 2.0 \mu\text{m}$ ). This study has shown that as expected, smaller particles contributed more to the total particulate count - particles sized 0.3, 0.5, 0.7, 1.0, 2.0

and 5.0  $\mu\text{m}$  had contributions of 85, 9.8, 4.0, 3.4, 1.6 and 0.3% respectively. While most measurements were conducted with a one-channel particle sampler that measures only  $\text{PM}_{10}$ , a small number of samples collected with a six-channel particle counter shows with certainty that  $\text{PM}_{10}$  is composed of particles sized 0.3  $\mu\text{m}$  and smaller, allowing for the implication that any high concentrations of particulates recorded contain correspondingly higher concentrations of particles  $\leq 0.3 \mu\text{m}$ .

Many literature sources cite airborne particulate standards and guidelines in mass form ( $\mu\text{g}/\text{m}^3$ ) rather than particle count form ( $\mu\text{m}/\text{m}^3$ ). For the purposes of comparing results to established standards, guidelines and other studies it was necessary to convert particle count measurements to a mass calculation. This study used a portable high volume air sampler along with particle counters to correlate particle counts with particle mass. These two parameters were correlated with an  $R^2$  of 0.62 allowing for the use of a regression trend line to predict the expected mass of a particle count. Using this method, it is shown that particle concentrations recorded match corresponding concentrations as reported in the literature and standards reported by the EPA and guidelines as established by the WHO.

Determining the chemical composition of local sediment or road dust is crucial to understanding the chemical composition of the coarse size fractions of PM, as coarse particulates are generally re-suspended material. Also, elemental composition of both urban and rural road dust coupled with enrichment factor calculations can help to attribute whether the sediment has been enriched by anthropogenic processes on either a regional (enrichment of urban sediment over

rural sediment) or global (enrichment of regional sediment over global crustal averages) scales.

This study used a FPXRF to analyze the chemical composition for collected road dust samples in urban and rural Phnom Penh. Chemical compositions were then used in enrichment factor calculations to determine the extent of enrichment of sediment as relating to background levels of rural locations. The study shows that urban road dust was not enriched over rural road dust by any means, and the rural road dust is suggested to be a source of material for the urban environment. Enrichment factor analysis also suggests that the urban sediment is a source for ambient material gathered by bulk collection methods.

Another crucial factor that must be understood to fully understand particulates in Phnom Penh is the influence of the seasons on particulate levels. Cambodia experiences two main seasons, the dry season (November-April) and the rainy monsoon season (May-October). Particle counts were collected at 88 points in the dry season and at a subset of 33 points in the following rainy season. Median fine and coarse particle counts dropped by 22% and 37% respectively over the course of the two sampling periods. This trend suggests that the rainy season experiences lower concentrations of PM when compared to the dry season. The monsoon rains experienced in the wet season help to wash particles from ambient air, while the rains also cause less vehicular traffic to be on the streets of Phnom Penh.

## **6.2 Recommendations for Further Study**

More detailed analysis of temporal particulate profiles is recommended. A valuable insight into the behavior of ambient PM would be ascertained by round-the-clock measurements, as limited equipment, personnel safety concerns were the main cause of the variable start and end times as seen in this study. Further studies should consider the possibility of real-time measurements perhaps provided by a series of permanent equipment installations incorporating many more measurement devices than this study was capable of (i.e. weather data and other air quality parameters). It is also suggested that further high volume air sampler studies should be carried out to expand upon the limited data set provided by this study. It is crucial to expand upon these measurements so that a larger data set more representative of other urban scenarios and weather and seasonal variations are taken into account. Further study of chemical composition is encouraged for airborne particulates. Analysis of particulates captured by the high volume air sampler is suggested to gain a better understanding of ambient fine particulates in Phnom Penh. It is also suggested that further studies be carried out between the variability of ambient PM in the dry and rainy seasons to better understand the overall impact of the seasons on particulate concentrations.

## References

- Aceves, M., Grimalt, J.O., 1993. Seasonally dependent size distributions of aliphatic and polycyclic aromatic hydrocarbons in urban aerosols from densely populated areas. *Environmental Science and Technology* 27: 2896-2908.
- Bernick, M.B., Kalinicky, D.J., Prince, G., Singhvi, R., 1995. Results of field-portable X-ray fluorescence analysis of metal contaminants in soil and sediment. *Journal of Hazardous Materials* 43: 101-110.
- Bergeslien, E., 2008. Personal Communication.
- BPA, 2008. How do Particle Counters Work? 28 Oct. 2008. <http://www.particlecounters.org/blog/how-do-particle-counters-work/>
- Central Intelligence Agency, 2008. World Fact Book – Cambodia. 28 Oct. 2008. <https://www.cia.gov/library/publications/the-world-factbook/geos/cb.html>
- Diner, D. J., Ackerman, T. P., Anderson, T. L., Bosenberg, J., Braverman, A. J., Charlson, R. J. et al., 2004. Paragon – An Integrated Approach for Characterizing Aerosol Climate Impacts and Environmental Interactions. *Bulletin of the American Meteorological Society* 85 (10): 1491-1501.
- Dasgupta, S., Deichmann, U., Meisner, C., Wheeler, D., 2005. Where is the Poverty-Environment Nexus? Evidence from Cambodia, Lao PDR, and Vietnam. *World Development* 33 (4): 617-638.
- Fang, G., Wu, Y., Chen, J., Rau, J., Huang, S., Lin, C. 2006. Concentrations of ambient air particulates (TSP, PM<sub>2.5</sub> and PM<sub>2.5-10</sub>) and ionic species at offshore areas near Taiwan Strait. *Journal of Hazardous Materials* B132: 269-276.
- Fraser, M.P., Yue, Z.W., Buzcu, B. 2003. Source apportionment of fine particulate matter in Houston, TX, using organic molecular markers. *Atmospheric Environment* 37: 2117-2123.
- Furuuchi, M., Murase, T., Yamashita, M., Oyagi, H., Sakai, K., Tsukawaki, S., Sieng, S., Hata, M., 2006. Temperature and Air Pollution in Phnom Penh, Cambodia – Influence of Land Use and the Mekong and Tonle Sap Rivers. *Aerosol and Air Quality Research* 6 (2): 134-149
- Fromme, H., Diemer, J., Dietrich, S., Cyrys, J., Heinrich, J., Lang, W., Kiranohlu, M., Twardella, D. 2008. Chemical and morphological properties of particulate matter (PM<sub>10</sub>, PM<sub>2.5</sub>) in school classrooms and outdoor air. *Atmospheric Environment* 42: 6597-6605.
- Garmin, 2008. eTrex® H. <https://buy.garmin.com/shop/shop.do?CID=144&PID=8705>

- Gehrig, R., Buchmann, B., 2003. Characterising seasonal variations and spatial distribution of ambient PM<sub>10</sub> and PM<sub>2.5</sub> concentrations based on long-term Swiss monitoring data. *Atmospheric Environment* 37: 2571-2580.
- Glover, D.M., Landsberger, H. and S., D'Auben, D.R., Vermette, S.J., 1989. Source Apportionment For Airborne Particles in Granite City, Illinois. Presented at Air & Waste Management Association 82<sup>nd</sup> Annual Meeting.
- Goldberg, M.S., Burnett, R.T., Bailar, J.C., Brook, J., Bonvalot, Y., Tamblyn, R., Singh, R., Valois, M.F., 2001. The association between daily mortality and ambient air particle pollution in Montreal, Quebec 1. Nonaccidental mortality. *Environmental Research* 86, 12–25.
- Gomiscek, B., Hauck, H., Stopper, S., Preining, O., 2004. Spatial and temporal variations of PM<sub>1</sub>, PM<sub>2.5</sub>, PM<sub>10</sub> and particle number concentration during the AUPHEP—project. *Atmospheric Environment* 38: 3917-3934.
- Harrison, R., Jones, M., Collins, G., 1999. Measurements of the physical properties of particles in the urban atmosphere. *Atmospheric Environment* 33: 309-321.
- Hettige, H., Huq, M., Pargal, S., Wheeler, D., 1996. Determinants of Pollution Abatement in Developing Countries: Evidence from South and Southeast Asia. *World Development* 24 (12), 1891-1904.
- Kim, C. S., Hu, S. C., De Witt, P., and Gerrity, T. R., 1996. Assessment of regional deposition of inhaled particles in human lungs by serial bolus delivery method. *Journal of Applied Physiology* 81: 2203–2213.
- Koulouri E., Saarikoski S., Theodosi C., Markaki Z., Gerasopoulos E., Kouvarakis G., Makela T., Hillamo R., Mihalopoulou N., 2008. Chemical composition and sources of fine and coarse aerosol particles in the Eastern Mediterranean. *Atmospheric Environment* 42: 6542-6550.
- Manoli, E., Voutsas, D., Samara, C., 2002. Chemical characterization and source identification/apportionment of fine and coarse air particles in Thessaloniki, Greece. *Atmospheric Environment* 36: 949-961.
- Lelieveld, J., Crutzen, P.J., Ramanathan, V., Andreae, M.O., Brenninkmeijer, C.A., Campos, T. et al., 2001. The Indian Ocean Experiment: Widespread Air Pollution from South and Southeast Asia. *Science* 291: 1031-1036.
- Martins, J.V., 2005. What is in the Air? *U.S. Air Quality – The Smog Blog*. 23 Oct. 2008. <http://alg.umbc.edu/usaq/archives/001044.html>
- Molyvann, V. 2003. *Modern Khmer Cities*, Reyum Publishing, Phnom Penh.
- Monkkonen, P., Uma, R., Srinivasan, D., Koponen, I.K., Lehtinen, K.E.J., Hameri, K. et al., 2004. Relationship and variations of aerosol number and PM<sub>10</sub> mass concentrations in a highly polluted urban environment—New Delhi, India. *Atmospheric Environment* 38: 425-433.

Niachou, K., Livada, I., Santamouris, M., 2008. Experimental study of temperature and airflow distribution inside an urban street canyon during hot summer weather conditions. Part II: Airflow analysis. *Building and Environment* 43: 1393-1403.

Thermo Scientific, 2007. Niton XLt/XLp/Xli 700 Product Specifications. 7 Nov. 2008. [http://www.niton.com/Documents/spec-sheets/7-204\\_0107\\_XLt-p-i\\_700\\_Spec\\_Sheet\\_web.pdf](http://www.niton.com/Documents/spec-sheets/7-204_0107_XLt-p-i_700_Spec_Sheet_web.pdf)

Peters, J.M., Avol, E., Navidi, W., London, S.J., Gauderman, W.J., Lurmann, F., Linn, W.S., Margolis, H., Rappaport, E., Gong, H., Thomas, D.C. 1999. A study of twelve southern California communities with differing levels and types of air pollution. I—Prevalence of respiratory morbidity. *American Journal of Respiratory and Critical Care Medicine* 159: 760–767.

Planning Department of Phnom Penh Municipality, 2004. Profiles of Phnom Penh City. 1 Dec. 2008. [http://www.phnompenh.gov.kh/english/PhnomPenh\\_Profile/E\\_PP\\_profile.pdf](http://www.phnompenh.gov.kh/english/PhnomPenh_Profile/E_PP_profile.pdf)

Pope, C.A., Dockery, D.W., Spengler, J.D., Raizenne, M.E. 1991. Respiratory health and PM10 pollution. *American Review of Respiratory Diseases* 144: 668–674.

Qian, Z., He, Q., Lin, H., Kong, L., Liao, D., Dan, J., Bentley, C, M., Wang, B. 2007. Association of cause-specific mortality with ambient particle air pollution in Wuhan, China. *Environmental Research* 105: 380-389.

Research Development Incorporated Cambodia, 2008. Arsenic research in Cambodia – Ground Water, Surface Water in Cambodia. 10 Dec. 2008. <http://www.rdic.org/waterarsenic.htm>

Reuters, 2001. Thousands ill as Phnom Penh air pollution doubles. 4 Mar. 2009. <http://www.planetark.org/dailynewsstory.cfm?newsid=11799>

Seames, W.S., 2003. An initial study of the fine fragmentation fly ash particle mode generated during pulverized coal combustion. *Fuel Processing Technology* 81: 109-125.

Seaton, A., MacNee, W., Donaldson, K., Godden, D. 1995. Particle air pollution and acute health effects. *The Lancet* 345: 176-178.

Seinfeld, J.H., 1986. Atmospheric Chemistry and Physics of Air Pollution. John Wiley & Sons, New York.

Schawrtz, J., Neas, L.M. 2000. Fine Particles Are More Strongly Associated than Coarse Particles with Acute Respiratory Health Effects in Schoolchildren. *Epidemiology* 11 (1): 6-10.

Soukup, J.M., Becker, S. 2001. Human Alveolar Macrophage Responses to Air Pollution Particulates Are Associated with Insoluble Components of Coarse Material, Including Particulate Endotoxin. *Toxicology and Applied Pharmacology* 171 (1): 20-26.

Spirn, A.W., 1984. The Granite Garden: Urban Nature and Human Design. Basic Books, New York.

- Srivastava, A., Jain, V.K., 2007. Size distribution and source identification of total suspended particulate matter and associated heavy metals in the urban atmosphere of Delhi. *Chemosphere* 68: 579-589.
- Stone, P., 2003. Dust, dust and some more dust, Phnom Penh, Cambodia. 4 Mar. 2009. <http://www.traveljournals.net/stories/2530.html>
- Takahiro, M., Masami, F., Shinji, T., Mitsuhiko, H., Michiko, Y., 2006. Present Status, Problems and Future Activities on Atmospheric Environmental Problems in South East Asian Developing Countries – Present Status and Characteristics of Ambient Air Pollution in Phnom Penh, Cambodia. *Journal of Aerosol Research* 21 (2): 101-107.
- Tippayawong, N., Pengchai, P., Lee, A., 2006. Characterization of ambient aerosols in Northern Thailand and their probable sources. *International Journal of Environment Science and Technology* 3 (4): 359-396.
- United Nations, 2002. Cambodia Country Profile. *Johannesburg Summit 2002*. <http://www.un.org/esa/agenda21/natinfo/wssd/cambodia.pdf>
- United Nations, 2005. Atmospheric/Air Pollution, Part III National Reporting Guidelines for CDS-14/15 Thematic Areas, UN Department of Economic and Social Affairs, Division of Sustainable Development. 10 Oct. 2008. <http://www.un.org/esa/agenda21/natinfo/countr/cambodia/atmosphere.pdf>
- United States Environmental Protection Agency. 2008. Office of Air and Radiation. 23 Oct. 2008. <http://www.epa.gov/air/>
- United States Environmental Protection Agency, 2007. Air Quality Management - National Ambient Air Quality Standards (NAAQS) for Criteria Pollutants. 23 Oct. 2008. <http://www.epa.gov/apti/course422/apc4a.html>
- Venkataraman, C., Thomas, S., Kulkarni, P., 1999. Size Distributions of Polycyclic Aromatic Hydrocarbons-Gas/Particle Partitioning to Urban Aerosols. *Journal of Aerosol Science* 30 (6): 759-770.
- Vermette, S.J., 2008. Personal Communication.
- Vermette, S.J., Irvine, K.N., Drake, J.J., 1988. Reciprocal Relations Between Urban Sediments and Precipitation Quality. *The East Lakes Geographer*: 23: 86-95
- Waller, R.E., 1967. Studies on the nature of air pollution. London Conference on Museum Climatology, International Institute for Renovation of Works of Art: 65-69.
- Wedepohl, K.H., 1971. Geochemistry. Holy, Rinehart and Winston, New York: 91.
- Wheeler, D. 2001. Racing to the Bottom? Foreign Investment and Air Pollution in Developing Countries. *Journal of Environment & Development* 10 (3): 225-245.

Wilson, W.E., Suh, H.H., 1997. Fine and coarse particles: concentration relationships relevant to epidemiological studies. *Journal of Air and Waste Management Association* 47: 1238-1249.

World Bank, 2005. Project Performance Assessment Report – Cambodia – Phnom Penh Power Rehabilitation Project.

[http://lnweb90.worldbank.org/oed/oeddoelib.nsf/DocUNIDViewForJavaSearch/1EB999EECEA2ECA385256FFE0066ABFB/\\$file/ppar\\_31663.pdf](http://lnweb90.worldbank.org/oed/oeddoelib.nsf/DocUNIDViewForJavaSearch/1EB999EECEA2ECA385256FFE0066ABFB/$file/ppar_31663.pdf)

World Health Organization, 2008. Air Quality and Health. 2 Oct. 2008.

<http://www.who.int/mediacentre/factsheets/fs313/en/>

Wu, Y., Fang, G., Lee, W., Lee, J., Chang, C., Lee, C. 2007. A review of atmospheric fine particulate matter and its associated trace metal pollutants in Asian countries during the period 1995-2005. *Journal of Hazardous Materials* 143: 511-515.